Department of Transportation
Research and Special Programs Administration
Office of Pipeline Safety

TTO Number 13

Integrity Management Program
Delivery Order DTRS56-02-D-70036

Potential Impact Radius Formulae for Flammable Gases Other Than Natural Gas Subject to 49 CFR 192

FINAL REPORT

Submitted by:
Michael Baker Jr., Inc.
June 2005

ChallengeUs.

This page intentionally left blank

TTO Number 13
Potential Impact Radius Formulae
for Flammable Gases Other Than Natural Gas

Table of Contents

List of Figures

List of Tables

Executive Summary

This report was prepared in accordance with the Statement of Work and proposal submitted in response to RFP for Technical Task Order Number 13 (TTO 13) entitled *"Potential Impact Radius Formulae for Flammable Gases Other Than Natural Gas."*

A key element of the Gas Integrity Management Rule (49 CFR 192, Subpart O) is the calculation of the potential impact radius (PIR) of a circle within which the potential failure of a pipeline could have significant impact on people or property.

The original derivation of the PIR formula referenced in 49 CFR 192 is contained in the Gas Research Institute (GRI) report by C-FER Technologies (C-FER), *"A Model for Sizing High Consequence Areas Associated with Natural Gas Pipelines"* (Stephens 2000). It must be recognized that this formula was derived solely on the premise that thermal radiation from a jet/trench fire is the dominant hazard related to pipe rupture and subsequent ignition. Since natural gas is non-toxic and significantly lighter than air, this premise is valid.

However, there are certain pipeline operators transporting flammable gases other than natural gas (e.g. hydrogen) that will be governed by the jet fire hazard, and thus there is a need for derivation of PIR formulae for use in identifying high consequence areas for these pipelines. While the C-FER report provides a basis for derivation of such formulae, the dimensionless values for emissivity factor, release rate decay factor, and efficiency factor used in the original derivation of the PIR formula have not been validated or optimized for flammable gases other than natural gas.

An introduction to this report is contained in Section 1, while Section 2 presents the more detailed background on the reasoning and assumptions used in the development of the PIR formulae presented in this report.

Section 3 documents the process utilized in identifying the various products that are known or reasonably assumed to be currently transported by pipelines in the US. Four products were chosen for PIR formula development: ethylene, hydrogen, rich natural gas and synthesis gas (syngas).

Section 4 comprises the majority of the report and describes the actual PIR formula development in a logical progression. At each step, the underlying formulae are given with the required variables presented and explained. This section concludes with a generalized methodology for use in determining the PIR for flammable gas mixtures. The PIR formula for natural gas referenced in 49 CFR 192 is also presented to allow the reader to compare the results of this study with the earlier work.

Section 5 describes the efforts conducted to validate the PIR formulae. These efforts were essentially fruitless due to the lack of actual incident data for the products of interest. Section 6 presents a commentary on the usage of constants for selected model factors that are in fact variables and would be treated as such if a more rigorous modeling approach were to be employed. Section 7 summarizes the results of the PIR formula development process. Finally, Section 8 presents a list of reference documents cited throughout the report.

The information included in the report that was entirely compiled by C-FER Technologies is contained in Appendix A.

This page intentionally left blank

1 Introduction

This report was prepared in accordance with the Statement of Work and proposal submitted in response to RFP for Technical Task Order Number 13 (TTO 13) entitled *"Potential Impact Radius Formulae for Flammable Gases Other Than Natural Gas"*.

A key element of the Gas Integrity Management Rule (49 CFR 192, Subpart O) is the calculation of the potential impact radius (PIR) of a circle within which the potential failure of a pipeline could have significant impact on people or property. Subpart O provides a specific formula for the calculation of the PIR that is to be used for natural gas:

$$r = 0.69 \cdot \sqrt{p \cdot d^2}$$

where:

r = the PIR in feet,

p = the pipeline maximum operating pressure in pounds per square inch, and

d = the nominal pipeline diameter in inches.

The original derivation of the above formula is contained in the Gas Research Institute (GRI) report by C-FER Technologies (C-FER), *"A Model for Sizing High Consequence Areas Associated with Natural Gas Pipelines"* (Stephens 2000). It must be recognized that this formula was derived solely on the premise that thermal radiation from a jet/trench fire is the dominant hazard related to pipe rupture and subsequent ignition. Since natural gas is non-toxic and significantly lighter than air, this premise is valid.

However, in the case of flammable gases that have a molecular weight comparable to air (i.e., a specific gravity near 1.0) or flammable gases that are also toxic, the jet fire thermal radiation hazard may not be the dominant hazard. If ignition is delayed for products with specific gravities near 1.0, these products can form a flammable vapor cloud of neutral buoyancy that will drift downwind until it encounters an ignition source. The size (or downwind extent) of the flammable cloud could exceed the jet fire thermal radiation hazard zone.

Similarly, gases that are toxic in addition to being flammable may have a broader impact due to dispersion without or prior to ignition.

However, there are certain pipeline operators transporting flammable gases other than natural gas (e.g. hydrogen) that will be governed by the jet fire hazard, and thus there is a need for derivation of PIR formulae for use in identifying high consequence areas for these pipelines. While the C-FER report provides a basis for derivation of such formulae, the dimensionless values for emissivity factor, release rate decay factor, and efficiency factor used in the original derivation of the PIR formula have not been validated or optimized for flammable gases other than natural gas.

This page intentionally left blank

2 Background

The failure of a high-pressure gas pipeline can lead to various outcomes, some of which can pose a significant threat to people and property in the failure location's immediate vicinity. For a given pipeline, the type of hazard that develops, and the damage or injury potential associated with the hazard, will depend on the mode of line failure (*i.e.*, leak vs. rupture), the nature of gas discharge (*i.e.*, vertical vs. inclined jet, obstructed vs. unobstructed jet) and the time to ignition (*i.e.*, immediate vs. delayed).

For gases with molecular weights significantly less than that of air (molecular weight of air is approximately 29 lbm/lb-mole), the possibility of a significant flash fire resulting from delayed remote ignition is extremely low since a low specific gravity usually precludes the formation of a persistent flammable vapor cloud at ground level. In these cases, the dominant hazard is thermal radiation from a sustained jet or trench fire, which may be preceded by a short-lived fireball.

In the event of line rupture, a mushroom-shaped gas cloud will form and then grow in size and rise due to discharge momentum and buoyancy. This cloud will, however, disperse rapidly and a quasi-steady gas jet or plume will establish itself. If ignition occurs before the initial cloud disperses, the flammable vapor will burn as a rising and expanding fireball before it decays into a sustained jet or trench fire. If ignition is slightly delayed, only a jet or trench fire will develop. Note that the added effect on people and property of an initial transient fireball can be quantified by overestimating the intensity of the sustained jet or trench fire that remains following the dissipation of the fireball.

A trench fire is essentially a jet fire in which the discharging gas jet impinges upon an opposing jet and/or the side of the crater formed in the ground. Impingement dissipates some of the momentum in the escaping gas and redirects the jet upward, thereby producing a fire with a horizontal profile that is generally wider, shorter and more vertical in orientation than a randomly directed and unobstructed jet would produce. The total ground area affected can, therefore, be greater for a trench fire than an unobstructed jet fire because more of the heat-radiating flame surface typically will be concentrated near the ground surface.

An estimate of the ground area affected by a credible worst-case failure event can, therefore, be obtained from a model that characterizes the heat intensity associated with rupture failure of the pipe where the escaping gas is assumed to feed a sustained trench fire that ignites very soon after line failure.

Because the size of the fire will depend on the rate at which fuel is fed to the fire, it follows that the fire intensity and the corresponding size of the affected area will depend on the effective rate of gas release. The release rate can be shown to depend on the pressure differential and the hole size. For guillotine-type failures, where the effective hole size is equal to the line diameter, the governing parameters would be the line diameter and the pressure at the time of failure. Given the wide range of actual pipeline sizes and operating pressures, a meaningful fire hazard model should explicitly acknowledge the impact of these parameters on the affected area.

This page intentionally left blank

3 Identify Flammable Gases Other than Natural Gas Subject to 49 CFR 192

3.1 Scope Statement

"Identify gases other than natural gas that are routinely transported by the pipeline industry and which would be subject to the requirements of 49 CFR 192, Subpart O. Identify and exclude from consideration products for which the dominant hazard may not be an ignited jet or trench fire. (This would include products for which the dominant hazard could be toxicity or fire, if the dominant fire hazard is associated with a ground-level vapor cloud.)"

3.2 Flammable Gases

Flammable gases are defined by the U.S. Department of Transportation under 49 CFR 115 Subpart D as:

> ...any material which is a gas at 20°C (68°F) or less and 101.3 kPa (14.7 psi) of pressure (a material which has a boiling point of 20°C (68°F) or less at 101.3 kPa (14.7 psi)) which-
>
> 1. Is ignitable at 101.3 kPa (14.7 psi) when in a mixture of 13 percent or less by volume with air; or
>
> 2. Has a flammable range at 101.3 kPa (14.7 psi) with air of at least 12 percent regardless of the lower limit.
>
> Except for aerosols, the limits specified in paragraphs (a)(1) and (a)(2) of this section shall be determined at 101.3 kPa (14.7 psi) of pressure and a temperature of 20°C (68°F) in accordance with ASTM E681-85, Standard Test Method for Concentration Limits of Flammability of Chemicals or other equivalent method approved by the Associate Administrator for Hazardous Materials Safety.

A general search for information regarding flammable gases yielded the list presented in Table 3.1. Sources references are also listed in this table:

- National Fire Protection Association (NFPA),
- The Pipeline Group, and
- Protection of Environment, Chemical Accident Prevention Provisions (40 CFR 68 Table 3).

Table 3.1 Flammable Gases

Product	Formula	Molecular Weight[1]	Governing Regulation	NFPA	The Pipeline Group	40 CFR 68	Comment
Acetylene	C_2H_2	26.04		X	X	X	Hydrocarbon
Aliene	C_3H_4	40.06		X			Hydrocarbon
Butadiene	C_4H_6	54.09		X	X	X	Hydrocarbon
Butane	C_4H_{10}	58.12	49 CFR 195	X	X	X	Hydrocarbon
Butene	C_4H_8	56.11		X	X	X	Hydrocarbon
Carbon Monoxide[2]	CO	28.01	49 CFR 192	X	X		
Carbonyl Sulfide	COS	60.07		X			
Cyanogen[2]	C_2N_2	52.04		X		X	
Cyclobutane	C_4H_8	56.11		X			Hydrocarbon
Cyclopropane	C_3H_6	42.08		X		X	Hydrocarbon
Deuterium	D_2	4.032		X			
Diborane[2]	B_2H_6	27.67		X			
Dimethyl Ether	$(CH_3)_2O$	46.07		X			Hydrocarbon
Dimethylamine	$(CH_3)NH$	45.08		X		X	Hydrocarbon
Dimethylpropane	$C(CH_3)_4$	72.15		X		X	Hydrocarbon
Ethane	C_2H_6	30.07	49 CFR 195	X	X	X	Hydrocarbon
Elthyl Acetylene	C_4H_6	54.09		X		X	Hydrocarbon
Elthyl Chloride	C_2H_5Cl	64.52		X		X	Hydrocarbon
Ethylene	C_2H_4	28.05	49 CFR 195	X	X	X	Hydrocarbon
Ethylene Oxide	C_2H_4O	44.05		X			Hydrocarbon
Genetron	Various[3]	Varies[3]		X			Refrigerant
Germaine[2]	GeH_4	76.62		X			
Hydrogen	H_2	2.016	49 CFR 192	X	X	X	
Hydrogen Selenide[2]	H_2Se	80.98		X			
Hydrogen Sulfide[2]	H_2S	34.08	49 CFR 192	X	X		
Isobutane	C_4H_{10}	58.12		X		X	Hydrocarbon
Isobutylene	C_4H_8	56.11		X			Hydrocarbon
Methane	CH_4	16.04	49 CFR 192	X	X	X	Hydrocarbon
Methyl Acetylene	C_3H_4	40.06		X			Hydrocarbon
Methyl Chloride	CH_3Cl	50.49		X			Hydrocarbon
Methyl Flouride	CH_3F	34.03		X			Hydrocarbon
Methyl Mercaptan[2]	CH_3SH	48.11		X			Hydrocarbon
Methyl Vinyl Ether	C_3H_9O	58.08		X			Hydrocarbon
Monomethylamine	CH_3NH_2	31.06		X			Hydrocarbon
Phosphine[2]	PH_3	34.00		X			
Propane	C_3H_8	44.10	49 CFR 195	X	X	X	Hydrocarbon
Propylene	C_3H_6	42.08	49 CFR 195	X	X	X	Hydrocarbon
Silane	SiH_4	32.11		X		X	
Tetrafluoroethylene	C_2F_4	100.02		X		X	
Trimethylamine[2]	$(CH_3)_3N$	59.11		X		X	Hydrocarbon
Vinyl Chloride	C_2H_3Cl	62.50		X		X	
Vinyl Flouride	C_2H_3F	46.04		X		X	

[1] Hydrocarbons with a molecular weight greater than ethylene (28.05) are assumed to be covered by 49 CFR 195 based on review of leak statistics for liquid lines provided on the OPS Web site.

[2] Toxic

[3] There are four variations listed on NFPA – Genetron-1113, Genetron-1132A, Genetron-142B and Genetron-152A

While no direct reference relating to the hydrocarbon gases was found in the codes and for which a governing code was not listed in Table 3.1, it is assumed that the majority of these are covered by 49 CFR 195. This assumption is based on a review of the molecular weights of the various gases that indicates all the hydrocarbon gases, with the exceptions of methane, and acetylene, are heavier than ethylene which is listed in the summary of leak statistics for liquids lines provided on the OPS Web site. In addition, the category *"Demethanized Mix"* is also referenced in the summary.

3.3 Gases Routinely Transported by Pipeline

A search of data housed within the National Pipeline Mapping System (NPMS) generated a short list of gases that are transported by pipeline (presented in Table 3.2). However, the broad category, "Other Gas", could cover numerous commodities, potentially both flammable and non flammable.

A range of nominal pipe sizes (NPS) associated with each gas identified in the NPMS and the governing regulations are also presented. Operators are not required to provide the NPS for inclusion into the NPMS, and the NPS default is zero. Thus in most cases, only the maximum listed NPS is shown.

Table 3.2 Gases Transported by Pipelines (from the NPMS)

Product	Governing Regulation	NPS
Anhydrous Ammonia	49 CFR 195	≤10
Carbon Dioxide	49 CFR 195	≤30
Hydrogen Gas	49 CFR 192	2 to 20
Natural Gas	49 CFR 192	Not available[1]
Other Gas	49 CFR 192	6 to 12

[1] The largest diameter gas pipeline listed by the American gas Association (AGA) is NPS 42.

A comparison of Table 3.1 and Table 3.2 yields a list of 14 flammable gases that might be subject to 49 CFR 192 based on the assumption regarding disposition of hydrocarbon gases discussed above. In addition, it was reported that ethylene, even though listed in the liquid pipelines incident reports, is sometimes transported through pipelines as a gas and was therefore also included for consideration. A list of the resulting 15 flammable gases is presented in Table 3.3.

Table 3.3 Flammable Gases Possibly Subject to 49 CFR 192

Product	Disposition
Acetylene	Common industrial gas, therefore PIR formula developed
Carbon Monoxide	Common industrial gas, therefore PIR formula developed
Carbonyl Sulfide	Considered uncommon and thus eliminated from further consideration
Deuterium	Considered uncommon and thus eliminated from further consideration
Diborane	Considered uncommon and thus eliminated from further consideration
Ethylene	Common industrial gas, therefore PIR formula developed
Genetron	Considered uncommon and thus eliminated from further consideration
Germane	Considered uncommon and thus eliminated from further consideration
Hydrogen Selenide	Considered uncommon and thus eliminated from further consideration
Hydrogen Sulfide	Common industrial gas, therefore PIR formula developed
Phosphine	Considered uncommon and thus eliminated from further consideration
Silane	Considered uncommon and thus eliminated from further consideration
Tetrafluoroethylene	Considered uncommon and thus eliminated from further consideration
Vinyl Chloride	Considered uncommon and thus eliminated from further consideration
Vinyl Flouride	Considered uncommon and thus eliminated from further consideration

The above list includes four gases that are common industrial gases: acetylene, carbon monoxide, ethylene and hydrogen sulfide. However, since carbon monoxide and hydrogen sulfide are also toxic and the heat of combustion is an order of magnitude less than that of methane, it is believed that the potential impact radius of a jet fire for these gases would be much less than the potential impact radius from the toxic cloud that may result due to a pipeline rupture. Therefore, these two gases were eliminated from further consideration in this report.

Acetylene was also eliminated since at a pressure around 30 psi, acetylene can polymerize explosively even without an admixture of air thus making it highly unlikely that acetylene is actually transported via pipelines subject to 49 CFR 192. References to acetylene pipelines found during research for this study indicate that existing systems operate at a pressure of 15 psi or less and are largely limited to industrial use such as shipyards for oxy-acetylene cutting and welding.

In addition, gases having a molecular weight near that of air (i.e., specific gravity near 1.0) may form a flammable vapor cloud of neutral buoyancy that can drift downwind until encountering an ignition source resulting in a short-lived flash fire (possibly having a much broader impact). Ethylene (specific gravity = 0.967) falls into this category, however, since OPS records indicate that there are pipelines transporting ethylene in a gaseous state, a PIR formula was developed for completeness.

Furthermore, since the PIR formula referenced by 49 CFR 192 was derived for pure methane, or "lean gas," "rich" natural gas was also chosen for formula development. Rich natural gas is natural gas containing significant quantities of the common heavier hydrocarbon gases, such as ethane, propane and butane. The composition of the rich natural gas mix considered is shown in Table 3.4.

Table 3.4 Rich Natural Gas Composition Considered

Compound	Composition (%)
Methane	80.0
Ethane	15.0
Propane	3.0
Butane	0.5
Nitrogen	0.5
Carbon Dioxide	0.5
Other	0.5
Total	100.0

Synthesis gas (syngas) is another form of gas that might be transported by pipeline. The European Industrial Gas Association (EIGA) describes syngas as a mixture of hydrogen (H_2) and carbon monoxide (CO), which may also contain significant, but lower, concentrations of methane (CH_4) and carbon dioxide (CO_2) as well as smaller amounts of impurities such as chlorides, sulfur compounds, and heavier hydrocarbons. The EIGA further defines syngas as a gaseous mixture containing at least 10 percent hydrogen and 200 parts per million (ppm) of carbon dioxide. Based on the broad range of possible compositions that might be considered syngas, the derivation of one simplified PIR formula becomes somewhat problematic. Obviously, if the mixture contains only hydrogen and carbon monoxide, then as the composition becomes more hydrogen-rich such a formula would approach a form identical to one derived for pure hydrogen; while as the composition becomes more carbon monoxide rich, the form would tend toward that for pure carbon monoxide. However, since methane may be present in significant quantities, such as with "coke" gas, the formula may tend toward the form derived for pure methane.

3.4 Summary

A total of four products were selected for which PIR formulae were developed:

- Ethylene
- Hydrogen
- Rich Natural Gas
- Syngas

The following sections present the PIR formula development process and describe the numerous variables used in the process.

Similar to syngas, there are potentially numerous other flammable gas mixtures or "mixed" gas (e.g., land-fill gas) for which the derivation of a single PIR formula may be unrealistic. Therefore, a methodology for calculation of an appropriate PIR for mixed gas composed of common elements is also presented.

4 Development of Potential Impact Radius Formulae

4.1 Scope Statement

"Develop a technically defensible technique for determining the potential impact radius that may result from an ignited rupture of a gas transmission line transporting flammable gases other than natural gas (as identified in Subtask 01). Determine the dimensionless values for the emissivity factor, release rate decay factor, and efficiency factor which should be used in the C-FER derivations of the potential impact radius formula for gases other than natural gas. Identify other parameters that are specific to the type of gas being assessed, such as molecular weight, specific heat ratio, and heat of combustion. The resulting models will be validated to the extent possible given relevant public domain incident data."

4.2 Heat Intensity Threshold

The original PIR formula derivation (Stephens 2000) used a heat intensity threshold of 5000 Btu/hr-ft^2 based on a review of several thermal load versus effect models. All of the models are based on an equation that relates the thermal load to a heat flux over time of the form:

$$L_p = t \cdot I^n \qquad \textbf{Equation 4.1}$$

where:

I = the heat flux;

L_p = the thermal load;

n = an index number; and

t = the exposure time.

The models used for the various injury limits are summarized in Table 4.1. The forms of these models are for use with metric units of heat flux (i.e., kW/m^2) with the time calculated in seconds.

Table 4.1 Thermal Load Versus Effect Models for Humans

Thermal Load Effect	Source	Equation
Time to Burn Threshold	Eisenberg et al. 1975	$t \cdot I^{1.15} = 195$
Time to Blister Threshold - Lower	Hymes 1983	$t \cdot I^{1.33} = 210$
Time to Blister Threshold - Upper	Hymes 1983	$t \cdot I^{1.33} = 700$
Time to 1% Mortality	Hymes 1983	$t \cdot I^{1.33} = 1060$
Time to 50% Mortality	Hymes 1983	$t \cdot I^{1.33} = 2300$
Time to 100% Mortality	Bilo & Kinsman 1997	$t \cdot I^{1.33} = 3500$

The results from the thermal load versus effect models given in the original report are reproduced in Table 4.2.

Table 4.2 Effects of Thermal Radiation on Humans

Heat Flux (Btu/hr ft^2)	1,600	2,000	3,000	4,000	5,000	8,000	10,000	12,000
Heat Flux (kW/m^2)	5.0	6.3	9.5	12.6	15.8	25.2	31.6	37.9
Time to Burn Threshold (sec)	30	23	15	11	8	5	4	3
Time to Blister Threshold – Lower (sec)	24	18	11	7	5	3	2	2
Time to Blister Threshold – Upper (sec)	81	60	35	24	18	10	7	6
Time to 1% Mortality (sec)	123	92	53	36	27	14	11	8
Time to 50% Mortality (sec)	267	198	116	79	59	31	23	18
Time to 100% Mortality (sec)	406	302	176	120	89	48	36	28

The exposure time adopted as the reference was 30 seconds based on the premise that an exposed person would stay in place for 1 to 5 seconds to evaluate the situation and then run at 5 miles per hour (7.3 feet per second) to some type of shelter within approximately 200 feet of their initial position. The exposure times closest to the reference time as estimated using the models described above are highlighted in Table 4.2 for each different thermal load effect category.

The heat intensity threshold of 5000 Btu/hr-ft^2 used in the original derivation was chosen by defining a significant chance of fatal injury as a 1% chance of mortality.

A similar approach was used to evaluate the potential of property (represented by a wooden structure) damage associated with a jet fire. Two scenarios were considered: piloted ignition (i.e., flame source present) and spontaneous ignition (i.e., no flame source present). The equation used had the form:

$$L_p = (I - I_x) \cdot t^n \qquad \textbf{Equation 4.2}$$

where:

I_x = the heat flux threshold below which ignition will not occur.

The actual models used are summarized in Table 4.3 and the results of the calculations are presented in Table 4.4.

Table 4.3 Thermal Load Versus Effect Models for Wood Structures

Thermal Load Effect	Source	Equation
Time to Piloted Ignition	Bilo and Kinsman 1997	$118.6 = (I - 14.7) \cdot t^{0.667}$
Time to Spontaneous Ignition	Bilo and Kinsman 1997	$167.6 = (I - 25.6) \cdot t^{0.8}$

Table 4.4 Effects of Thermal Radiation on Wooden Structures

Heat Flux (Btu/hr ft^2)	Heat Flux (kW/m^2)	Time to Piloted Ignition (sec)	Time to Spontaneous Ignition (sec)
4,000	12.6	No ignition	No ignition
5,000	15.8	1162	No ignition
8,000	25.2	38	No ignition
10,000	31.6	19	65
12,000	37.9	12	26

As illustrated in Table 4.4, for a heat flux of 5000 Btu/hr-ft^2 piloted ignition will occur after approximately 20 minutes (1162 sec), but spontaneous ignition is not possible. The C-FER report states: "…this heat intensity represents a reasonable estimate of the heat flux below which wooden structures would not be destroyed, and below which wooden structures should afford indefinite protection to occupants."

4.3 Fire Model

As discussed in the C-FER report (Stephens 2000), the heat flux, *I*, at a given distance from a jet flame can be characterized by the formula:

$$I = \frac{\mu \cdot X_g \cdot Q_{eff} \cdot H_c}{4 \cdot \pi \cdot r^2} \qquad \textbf{Equation 4.3}$$

where:

H_c = heat of combustion

μ = efficiency factor (the symbol η is used in the original GRI report by C-FER and in the C-FER report presented in Appendix A of this document)

X_g = emissivity factor

Q_{eff} = effective release rate

r = horizontal distance from heat source

The variables in the above formula are discussed in further detail in the following sections. The complete C-FER Technologies report documenting the development of the emissivity and efficiency factors is also included as Appendix A.

4.4 Emissivity Factor

The emissivity factor (dimensionless) in Equation 4.3 acknowledges that only a fraction of the heat energy theoretically released by combustion is dissipated through radiation. In general, the fraction of combustion energy radiated will depend on the efficiency of the combustion process, the tendency for the resulting flame to produce soot, and the magnitude of heat lost by convection to the entrained air. The emissivity factor, also referred to in the literature as the 'radiant fraction', is product dependent. However, the discharge velocity and overall size of the fire can also have a significant

influence on the fraction of heat radiated. Discharge velocity is important because an increasing velocity is associated with a progressive increase in the degree of air-fuel mixing, which increases the proportion of heat lost to convection (Brzustowski et al 1975, Chamberlain 1987). The size of the fire is important because larger fires are associated with longer flame residence times and an increased residence time increases the fraction of heat that can be radiated (Becker and Liang 1982, Schefer et al. 2004).

Estimates of the radiant fraction reported in the literature are predominantly associated with small flares discharging at relatively low speeds (i.e. jets with velocities well below the sonic velocity). These values are generally assumed to provide reasonable estimates of the fraction of the heat radiated during controlled gas flaring operations, however, they are potentially inappropriate for use in assessing the heat radiated by a fire resulting from pipeline rupture, which can produce a very large flame and typically involves gas discharge under very high speed (i.e. sonic) conditions.

The emissivity factor (or radiant fraction) to be used in the fire model for a given product is the value applicable to relatively low speed (i.e. subsonic) jets, which would commonly be employed in flaring system design. To make it more applicable to the estimation of the radiant heat energy produced by sonic jets feeding large-scale fires, an adjustment to this reference emissivity value is incorporated in the radiation efficiency factor (see Section 4.5).

A literature survey was carried out to compile estimates of the radiant fraction for a range of hydrocarbon and non-hydrocarbon fuel sources. As noted, most of the available information comes from small-scale fire tests. The small-scale test data is summarized in Appendix A, Table A.1. Note that many references cite estimates of the radiant fraction that are directly or indirectly attributable to the early experiments of Zabetakis and Burgess (1961); only data from original sources is included in the table. Note also that the tabulated values are, in all cases, the maximum or upper plateau values recorded during the tests. Where testing programs also involved high-speed jets, all researchers reported a significant reduction in the radiant fraction with increasing jet velocity.

Some large-scale fire test data is available for releases involving natural gas. Work by Chamberlain (1987) and Cook et al. (1987) indicates that the effective radiant fraction for natural gas flares falls in the range of 0.34 to 0.07 with both studies clearly demonstrating that the radiant fraction falls with jet velocity. Best-fit relationships developed from the test data by these researchers suggest that for jet velocities in the range typical of conventional flaring operations (i.e. velocities in the range of Mach 0.2 to 0.5), the effective radiant fraction is in the range of 0.3 to 0.2, and under sonic discharge conditions (i.e. velocities above Mach 1.0) the radiant fraction falls below 0.16. This finding is particularly important because as previously noted, under typical operating conditions, pipeline ruptures will always be associated with sonic discharge conditions.

Suggested emissivity factors for products of interest, developed from the above information, are given in Table 4.5.

Table 4.5 Emissivity Factors

Product	Factor
Ethylene	0.35
Hydrogen	0.15
Lean Natural Gas (Methane)	0.20
Rich Natural Gas	0.20
Syngas	0.15 (≤10% CH_4) 0.20 (>10% CH_4)

With regard to lean natural gas, it is noted that the emissivity factor of 0.2, cited in the derivation of the original PIR formula, may appear somewhat non-conservative in light of the work by Chamberlain and Cook et al. described above; however, as previously noted, the emissivity factors are effectively adjusted downwards (through the efficiency factor) to reflect conditions appropriate to sonic discharge events involving large-scale fires (see Section 4.5).

Note that for rich natural gas, it is assumed that the emissivity is comparable to that of lean gas because the fractions of ethane and propane involved in a rich natural gas mixture are not substantial and because the reference emissivity values of the major components of rich natural gas are similar.

4.5 Efficiency Factor

The efficiency factor (dimensionless) is intended to address a number of conservatisms inherent in the simplified form of the model originally developed to estimate radiation intensity as a function of distance from the fire source. Specifically, it accounts for the conservatism associated with:

- ignoring the atmospheric absorption of a portion of the radiant energy;
- the simplified treatment of flame geometry and opacity; and
- the fact that the commonly cited emissivity factors would generally overestimate a flame that develops in the event of a pipeline rupture.

The efficiency factor is somewhat product dependent.

4.5.1 Basis for the Efficiency Factor

To understand the basis for the efficiency factor incorporated in the original model, it is necessary to consider a more refined point source radiation model that explicitly addresses the effects noted above.

Such a model, as adapted from a widely recognized flare radiation model developed by Cook et al. (1987), takes the form:

$$I = Q_{eff}\, H_c\, X_g^*\, \tau\, F_p \qquad \textbf{Equation 4.4}$$

where:

Q_{eff} = effective sustained gas release rate (kg/s);

H_c = heat of combustion (J/kg);

X_g^* = effective emissivity factor, adjusted for discharge velocity and fire size,

τ = atmospheric transmissivity; and

F_p = point source view factor (/m^2).

The effective emissivity factor is given by:

$$X_g^* = X_g\, C_{Xg} \qquad \textbf{Equation 4.5}$$

where:

X_g = emissivity factor under conventional flaring conditions (see Section 4.4), and

C_{Xg} = emissivity adjustment factor.

The view factor is given by:

$$F_p = A_{iso}\, F_{iso} + (1 - A_{iso}) F_{dif} \qquad \textbf{Equation 4.6}$$

where A_{iso} is an empirically derived constant that determines the relative applicability of isotropic versus diffuse emission assumptions. Large-scale experiments with natural gas flames led Cook et al. to conclude that the best correlation between predicted and actual radiation levels in both the near and far field is achieved using a value of A_{iso} equal to 0.5.

Isotropic emission assumes an optically thin flame that is effectively transparent to radiation in all directions. The associated view factor is:

$$F_{iso} = \frac{1}{4\pi x^2} \qquad \textbf{Equation 4.7}$$

where x is the line of sight distance (in meters) from the center of the flame to the point of interest.

Diffuse emission assumes the flame is completely opaque, radiating only from the surface envelope. The associated view factor is:

$$F_{dif} = \frac{\cos\theta}{4\pi x^2} \qquad \textbf{Equation 4.8}$$

where θ is angle subtended by the normal to the flame locus at the point source and the line joining the point source to the target.

If the flame is assumed to be vertically oriented, and if it is further idealized as a single point source emitter located at flame mid-height, the fire geometry takes the general shape shown in Figure 4.1.

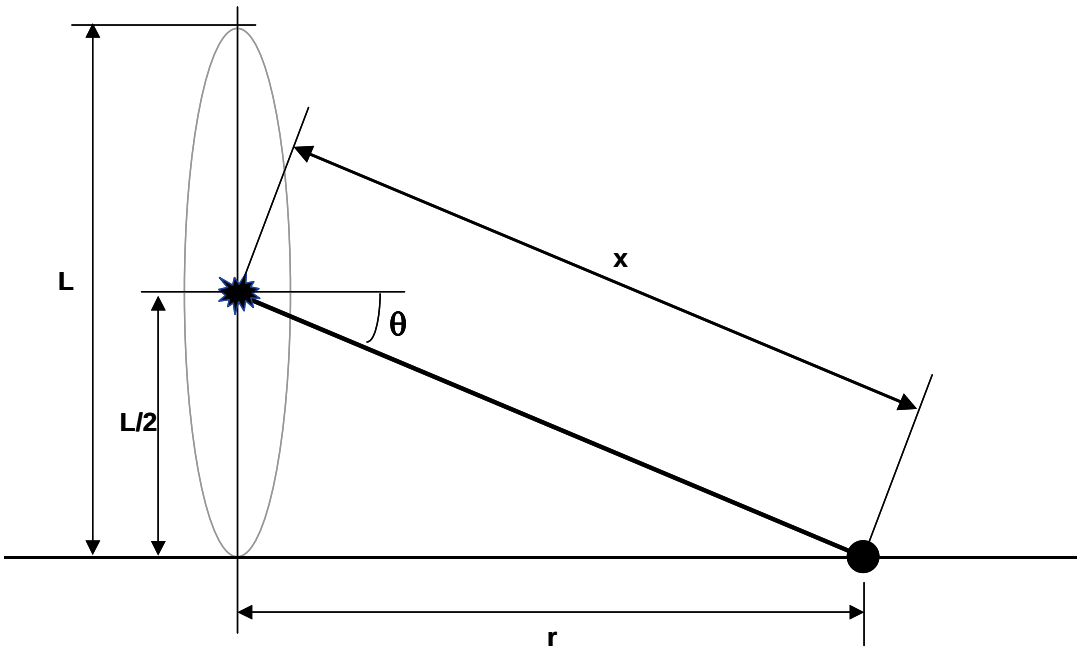

Figure 4.1 Elevated Point Source Fire Model Geometry

From Figure 4.1 it follows that the relationship between the line of sight distance *x* and the horizontal distance projection *r* is given by

$$x = \frac{r}{\cos\theta} \qquad \textbf{Equation 4.9}$$

where the view angle θ is given by:

$$\theta = \arctan\left(\frac{L/2}{r}\right) \qquad \textbf{Equation 4.10}$$

Substituting Equations 4.5 through 4.9 into Equation 4.4, the resulting point source radiation model is:

$$I = \frac{X_g\, C_{Xg}\, \tau\, Q_{eff}\, H_c}{4\pi r^r} \cos^2\theta\left(0.5 + 0.5\cos\theta\right) \qquad \textbf{Equation 4.11}$$

Comparison of the radiation intensity model given by Equation 4.11 with the point source model used in the original derivation of the PIR formula by C-FER as given by Equation 4.3 shows that the two are equivalent if the efficiency factor in the original model is equal to:

$$\mu = C_{Xg}\, \tau \cos^2\theta\left[0.5 + 0.5\cos\theta\right] \qquad \textbf{Equation 4.12}$$

To quantify the efficiency factor, estimates are required of the view angle θ, the atmospheric transmissivity τ, and the emissivity adjustment factor C_{Xg}.

4.5.2 View angle

To estimate the view angle, an estimate of the flame length is required. For large-scale hydrocarbon fires, the flame length can be estimated using the GRI flame length model (Atallah and Saxena 1995). This empirical model was developed through regression analysis of data from pipeline failure reports published by the National Transportation Safety Board, the results of large-scale experiments on natural gas and LPG published in the literature, and observations made during oil well fires. According to this model, the flame length (in meters) is given by:

$$L = 0.0274\left(Q_{eff}\, H_c\right)^{0.352} \qquad \textbf{Equation 4.13}$$

For a given release scenario, Equation 4.13, in conjunction with Equations 4.10 and 4.11, can be used to estimate the view angle. Note that the interdependence of the parameters in these equations makes this an iterative calculation process. It also requires an estimate of the atmospheric transmissivity τ, and the emissivity adjustment factor C_{Xg}.

4.5.3 Atmospheric Transmissivity

A portion of the heat energy radiated from a fire is absorbed and scattered by the atmosphere causing a reduction in the radiation received by targets at some distance from the flame. The amount of radiation lost to the atmosphere depends on the wavelength of the radiation, the amount of water vapor in the atmosphere, and the distance traveled. For hydrocarbon fires, which radiate a significant portion of their heat within the visible spectrum (i.e. luminous flames), these radiation losses typically range between 10% and 40%.

Atmospheric transmissivity is a measure of the fraction of radiant energy reaching a target. Numerous models are available for estimating the transmissivity of radiation from luminous flames. A widely cited formula (Bagster and Pitblado 1989) is:

$$\tau = 2.02\,(P_w\, x)^{-0.09} \qquad \textbf{Equation 4.14}$$

where

P_w = partial pressure of water vapor in the atmosphere (Pa); and

x = line of sight distance (m).

The partial pressure of water vapor is a function of air temperature and humidity level, which can be estimated by the formula:

$$P_w = RH\, P_w^0 = RH\,(610.7 x 10^{[7.5T/(237.3+T)]}) \qquad \textbf{Equation 4.15}$$

where

P_w^0 = saturated vapor pressure of water in the atmosphere (Pa);

RH = relative humidity (fraction); and

T = air temperature (°C).

When atmospheric transmissivity is to be estimated in a generic sense, it is common to assume an air temperature and relative humidity that is associated with a conservatively low estimate of the level of water vapor in the atmosphere, because a low water vapor content is associated with a higher transmissivity.

For products that produce fires radiating primarily outside the visible spectrum (i.e., nonluminous flames), the usual hydrocarbon fire transmissivity models are not applicable. Examples of products producing a largely invisible flame include: hydrogen, synthesis gases (i.e., syngas) for which the dominant constituents are a mixture of hydrogen and carbon monoxide, and methanol. Unfortunately, limited information is available on the transmissivity of nonluminous flames over significant distances. The only directly relevant information found in the literature is a hydrogen fire transmissivity formula developed over 40 years ago by Zabetakis and Burgess (1961). This model takes the form:

$$\tau = e^{-0.0492\,w\,x} \qquad \textbf{Equation 4.16}$$

where

w = water content of the atmosphere (% by weight); and

x = line of sight distance (m).

The water content by weight percent is given by

$$w = 6.2x10^{-4}\,P_w \qquad \textbf{Equation 4.17}$$

where

P_w is given by Equation 4.15.

If the air temperature is assumed to be 15°C, consistent with the assumption made in developing the original PIR formula, and the relative humidity is assumed to be 40%, the atmospheric transmissivity versus line of sight distance for luminous (hydrocarbon) and nonluminous (hydrogen) flames are as shown in Figure 4.2.

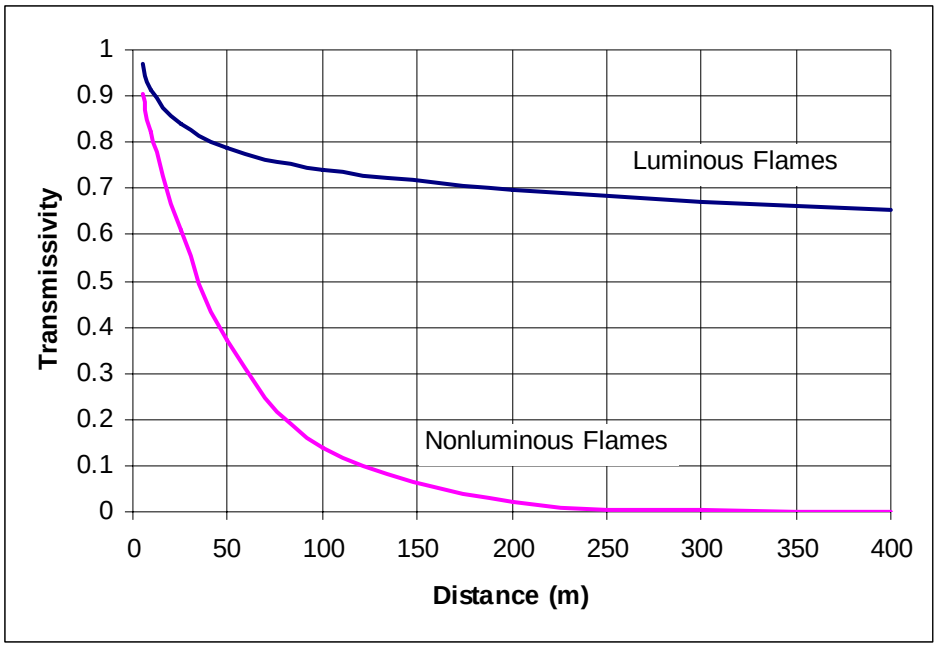

Figure 4.2 Transmissivity Comparison for Luminous and Nonluminous Flames

Based on the information discussed above, the transmissivity of the atmosphere to radiation from nonluminous hydrogen flames falls much more rapidly with distance than does the transmissivity for luminous hydrocarbon flames.

It is noted that the relationship developed by Zabetakis and Burgess was based on laboratory scale experiments and limited fire testing. The validity of this model for estimating transmissivity over significant distances is therefore not as well established as the model presented for luminous flames. However, the relationship indicated by the model is supported by anecdotal information that indicates the major concern with hydrogen fires being they are difficult to see (i.e. the flame is nearly invisible) and the rapid attenuation of radiation by the atmosphere makes it difficult for a person to gauge distance to the flame face. This anecdotal information suggests that the dominant hazard to people is inadvertent direct exposure to the flame rather than thermal radiation at a distance. As discussed later, this presents a significant problem when trying to characterize the hazard zone for products that produce nonluminous flames.

4.5.4 Emissivity Adjustment

As discussed in Section 4.4, the emissivity factor to be used in the fire model is the commonly cited emissivity level applicable to controlled gas flaring operations. Also as discussed, these emissivity levels are not considered directly applicable to large fires produced by gas jets discharging at high velocities. Thus, an adjustment is considered appropriate when taking into account radiation from pipeline rupture fires, which can be very large and are typically associated with sonic discharge conditions during the early stages of a release event.

Unfortunately, limited information is available on the emissivity of large-scale fires fed by sonic jets. The best information available pertains to natural gas. Large-scale flare test data reported by Chamberlain (1987) and Cook et al. (1987) suggests that for jet velocities at or above the sonic velocity of natural gas, the measured emissivity of the flame is at least 25% to 50% lower than the emissivity measured at low velocities. In addition, best-fit relationships developed by these researchers indicate that at jet velocities at or above the sonic velocity, the actual emissivity is below 0.16. Based on this information, an emissivity adjustment factor of $C_{Xg} = 0.75$ is considered appropriate for natural gas. This reduces the emissivity of natural gas from the assumed reference value of 0.2 to an effective value of 0.15, which compares favorably with the values given by the regression models developed by both Chamberlain and Cook et al.

No comparable information is available for other products. However, as noted in Section 4.4, small-scale test data indicates that all products of interest exhibit a reduction in emissivity with increased jetting velocity. In the absence of product-specific data, the emissivity adjustment factor adopted for natural gas is assumed to be applicable to all products of interest.

4.5.5 Efficiency Factor for Lean Natural Gas

Following the approach described above, estimates of the radiation efficiency factor, consistent with the refined thermal radiation hazard model, can be developed for natural gas pipelines over a range of diameter-pressure combinations. The values obtained for lean natural gas, as represented by the properties of methane, are summarized in Table 4.6.

Table 4.6 Efficiency Factors for Lean Natural Gas Pipelines

Diameter d (in)	Press. p (psi)	Power $Q_{eff}\,H_c$ (kJ/s)	Zone Radius r (m)	Flame Height L (m)	View Angle θ (deg)	Sight Dist. x (m)	Atmos. Trans. τ	Emissivity Adjust. C_{Xg}	Efficiency Factor μ
6.625	500	2.71×10^6	23.2	57.3	51.0	36.9	0.812	0.75	0.197
12.75	750	1.51×10^7	70.5	105	36.6	87.9	0.751	0.75	0.327
24	1000	7.12×10^8	165	181	28.8	188	0.701	0.75	0.379
36	1250	2.00×10^8	283	261	24.8	311	0.670	0.75	0.395
42	1500	3.27×10^8	363	310	23.1	395	0.656	0.75	0.399
								Average→	0.34

Assumed lean gas properties (100% CH_4): M = 16.04 g/mol, γ = 1.306, H_c = 50,000 kJ/kg
Hazard zone radius calculated assuming:
- heat intensity threshold = 15.77 kW/m^2
- emissivity factor = 0.2
- release rate decay factor = 0.33

The results given in Table 4.6 indicate that the efficiency factor used in the development of the original model (i.e. $\mu = 0.35$) is conservative for small diameter, low-pressure pipelines and slightly non-conservative for large diameter, high-pressure lines. Given the range and central tendency of the tabulated estimates of the efficiency factor, the adopted reference value is shown to be a reasonable single valued approximation to the range of efficiency factors that apply to the natural gas pipeline population as a whole.

4.5.6 Products Associated with Luminous Flames

4.5.6.1 Rich Natural Gas

For a rich natural gas, the efficiency factor estimates obtained using the approach described above are summarized in Table 4.7 for a representative range of diameter-pressure combinations.

Table 4.7 Efficiency Factors for Rich Natural Gas Pipelines

Diameter d (in)	Press. p (psi)	Power Q_{eff} H_c (kJ/s)	Zone Radius r (m)	Flame Height L (m)	View Angle θ (deg)	Sight Dist. x (m)	Atmos. Trans. τ	Emissivity Adjust. C_{Xg}	Efficiency Factor μ
6.625	500	3.11×10^6	25.8	60.1	49.4	39.6	0.806	0.75	0.212
12.75	750	1.73×10^7	76.2	110	35.8	94.0	0.746	0.75	0.333
24	1000	8.16×10^8	177	190	28.2	201	0.697	0.75	0.382
36	1250	2.30×10^8	303	273	24.3	333	0.666	0.75	0.397
42	1500	3.75×10^8	389	325	22.7	422	0.652	0.75	0.400
								Average→	0.35

Assumed rich natural gas properties (80% CH_4, 15% C_2H_6, 3% C_3H_8, 0.5% C_4H_{10}, 2.5% other):
M = 19.48 g/mol, γ = 1.29, H_c = 47,886 kJ/kg
Hazard zone radius calculated assuming:
- heat intensity threshold = 15.77 kW/m^2
- emissivity factor = 0.2
- release rate decay factor = 0.36

The results indicate that the efficiency factor developed for lean natural gas (μ = 0.35) is equally applicable to rich natural gas. This is because the chemical power associated with rupture failure (i.e. the product of Q_{eff} and H_c) is similar for both lean and rich natural gases and the emissivity or radiant fraction for both product mixtures is essentially the same.

4.5.6.2 Ethylene

For ethylene, the calculated efficiency factor estimates are summarized in Table 4.8. The adopted diameter-pressure range differs from the range used for natural gas pipelines. A smaller diameter range was used because it is considered more representative of refined product pipelines. The results suggest that an efficiency factor of 0.4 is more appropriate for this product.

Table 4.8 Efficiency Factors for Ethylene Pipelines

Diameter d (in)	Press. p (psi)	Power Q_{eff} H_c (kJ/s)	Zone Radius r (m)	Flame Height L (m)	View Angle θ (deg)	Sight Dist. x (m)	Atmos. Trans. τ	Emissivity Adjust. C_{Xg}	Efficiency Factor η
4.5	500	1.43×10^6	29.2	45.8	38.1	37.1	0.811	0.75	0.337
12.75	1000	2.30×10^7	131	122	24.9	144	0.718	0.75	0.422
20	1500	8.48×10^8	254	193	20.8	271	0.678	0.75	0.430
								Average→<	0.40

Assumed ethylene properties: M = 28.54 g/mol, γ = 1.22, H_c = 47,162 kJ/kg
Hazard zone radius calculated assuming:
- heat intensity threshold = 15.77 kW/m^2
- emissivity factor = 0.35,
- release rate decay factor = 0.31

4.5.7 Products Associated with Nonluminous Flames

If it is assumed that the atmospheric transmissivity relationship given by Zabatekis and Burgess for hydrogen flames (see Section 4.5.3) is applicable to nonluminous flames in general, the rapid attenuation of thermal radiation with distance (see Figure 4.2) presents a problem when trying to apply the fire hazard model (see Section 4.3) to pipelines transporting hydrogen and other products that produce nonluminous flames (e.g., syngas, etc.). The original PIR formula was developed assuming the dominant hazard is thermal radiation, and radiation intensity will remain significant well beyond the flame face. This is fundamental to the hazard zone radius estimation procedure. If radiation intensity away from the flame face is low due to rapid attenuation by the atmosphere, then the radiation hazard area will collapse to a size significantly less than the flame length and become secondary to the hazard posed by direct exposure to the flame.

In an attempt to address the flame exposure hazard using the existing thermal radiation hazard model framework, it is proposed that the hazard zone radius be defined in a manner to be comparable to the length of a possible directed jet. Unfortunately, difficulties exist for this method as well, since a proven model for estimating the length of large-scale hydrogen flames is not yet available. As an interim approach, it is proposed that the efficiency factor for nonluminous flames be chosen to ensure the hazard zone radius obtained from the fire model is comparable to the flame length estimated using Equation 4.13, assuming that for a directed jet the mass flow feeding the flame is the discharge from a single end of the pipe (i.e. use 1/2 Q_{eff} in Equation 4.13).

The length of a directed jet, as calculated using Equation 4.13 with a reduced effective mass flow rate, is shown in comparison to the hazard zone radius given by the existing hazard zone model in Table 4.9, for a range of hydrogen pipeline diameter-pressure combinations. Similar results are given for syngas pipelines in Table 4.10. It is shown in both tables that the zone radius is comparable to the flame length if the value of the efficiency factor proposed in the original model is retained. Thus, the value of the efficiency factor originally proposed for natural gas is recommended for hydrogen and syngas.

Table 4.9 Hazard Zone Radius versus Directed Jet Length for Hydrogen Pipelines

Diameter d (in)	Press. p (psi)	Total Power Q_{eff} H_c (kJ/s)	Zone Radius* r (m)	Half Power ½*Q_{eff} H_c (kJ/s)	Directed Jet Length L (m)
6.625	500	1.72×10^6	21.4	8.62×10^5	38.3
12.75	750	9.58×10^6	50.4	4.79×10^6	70.0
24	1000	4.53×10^7	110	2.26×10^7	121
36	1250	1.27×10^8	184	6.37×10^7	174
42	1500	2.08×10^8	235	1.04×10^8	207

Assumed hydrogen properties: M = 2.016 g/mol, γ = 1.412, H_c = 120,000 kJ/kg
Zone radius calculated assuming:
- heat intensity threshold = 15.77 kW/m^2
- efficiency factor = 0.35
- emissivity factor = 0.15,
- release rate decay factor = 0.24

Table 4.10 Hazard Zone Radius versus Directed Jet Length for Syngas Pipelines

Diameter d (in)	Press. p (psi)	Total Power Q_{eff} H_c (kJ/s)	Zone Radius* r (m)	Half Power ½*Q_{eff} H_c (kJ/s)	Directed Jet Length L (m)
6.625	500	7.72×10^5	14.3	3.86×10^5	28.5
12.75	750	4.29×10^6	33.7	2.14×10^6	52.8
24	1000	2.03×10^7	73.2	1.01×10^7	91.1
36	1250	5.70×10^7	123	2.85×10^7	131
42	1500	9.30×10^7	157	4.65×10^7	156

Assumed syngas properties (50% H_2, 50% CO): M = 15 g/mol, γ = 1.41, H_c = 17,400 kJ/kg
Zone radius calculated assuming:
- heat intensity threshold = 15.77 kW/m^2
- efficiency factor = 0.35
- emissivity factor = 0.15,
- release rate decay factor = 0.27

4.5.8 Summary of Efficiency Factors

The recommended efficiency factors for products of interest, developed as described above, are summarized in Table 4.11.

Table 4.11 Efficiency Factors

Product	Factor
Ethylene	0.40
Hydrogen	0.35
Lean Natural Gas (Methane)	0.35
Rich Natural Gas	0.35
Syngas	0.35

4.6 Effective Release Rate Model

The peak release rate, Q_{in}, from a single side of a guillotine line rupture can be estimated using the gas discharge equation for sonic or choked flow through an orifice:

$$Q_{in} = C_d \cdot \frac{\pi \cdot d^2}{4} \cdot p \cdot \frac{\varphi}{a_0} \qquad \textbf{Equation 4.18}$$

where:

$$\varphi = \text{flow factor} = \gamma \cdot \left(\frac{2}{\gamma + 1} \right)^{\frac{\gamma+1}{2\cdot(\gamma-1)}}; \qquad \textbf{Equation 4.18a}$$

$$a_0 = \text{sonic velocity of gas} = \sqrt{\frac{\gamma \cdot R \cdot T}{m}}; \qquad \textbf{Equation 4.18b}$$

γ = specific heat ratio of gas;

R = gas constant of gas;

T = initial temperature of gas in the pipeline;

m = molecular weight of gas;

C_d = discharge coefficient;

d = effective hole diameter (line diameter for guillotine cut);

p = pressure differential (line pressure).

A guillotine-type failure of a pipeline will normally result in double-ended release, in which case the effective release rate feeding a steady-state fire would be:

$$Q_{eff} = 2 \cdot \lambda \cdot Q_{in} = 2 \cdot \lambda \cdot C_d \cdot \frac{\pi \cdot d^2}{4} \cdot p \cdot \frac{\varphi}{a_0} \qquad \textbf{Equation 4.19}$$

where:

λ = release rate decay factor, and

the factor 2 accounts for the gas escaping from both sides of the guillotine break.

4.7 Release Rate Decay Factor

The release rate decay factor in Equation 4.19 is a convenient method to approximate the energy released over a period of time, 30 seconds in this case as discussed in Section 4.2. This will be discussed further later in this section. In order to determine an appropriate release decay factor, it is first necessary to evaluate the relative release rate versus time. There are numerous methods that can be used to estimate release rate versus time for discharges from pressurized systems. However, many of these methods are applicable to releases from tanks and cylinders, and do not account for frictional work within the pipeline; therefore caution must be used to ensure that an appropriate method is used.

The original derivation of the PIR formula given in 49 CFR 192 was completed using a non-dimensional rate decay model presented in a study by the Netherlands Organization of Applied Scientific Research, Division of Technology for Society (TNO 1982). This model "is based on realistic gas flow and decompression characteristics and which acknowledges both the compressibility of the gas and the effects of pipe wall friction," (Stephens 2000). In order to ensure consistency with the original derivation, the same approach is used in this study.

The TNO report concludes that the ratio of the mass flow at a given point in time and the initial rate of flow (denoted the "reduced" release rate) is inversely proportional to the cube root of the time from rupture and the ratio between the Fanning friction factor and the pipe diameter, and is given by the equation:

$$m_r = (1 + 0.75 \cdot t_r)^{-1/3}$$ **Equation 4.20**

where:

t_r = the "reduced" time given by:

$$t_r = t \cdot \left(\frac{f}{2 \cdot d}\right) \cdot \sqrt{\frac{z_u \cdot R \cdot T}{m}}$$ **Equation 4.21**

where:

f = friction factor;

t = time from rupture; and

z_u = compressibility factor of the gas.

The friction factor is calculated using the Colebrook and White formula:

$$\sqrt{\frac{1}{f}} = -2 \cdot \log\left(\frac{2.51}{\mathrm{Re} \cdot \sqrt{f}} + \frac{K}{3.71 \cdot d_i}\right)$$ **Equation 4.22**

where:

d_i = inside diameter of the pipe;

K = the absolute surface roughness of the pipe wall (assumed 0.00063 in/in); and

Re = the Reynolds number.

In high-pressure pipelines, the quantity $\frac{K}{3.71 \cdot d_i}$ is normally much larger than $\frac{2.51}{\mathrm{Re} \cdot \sqrt{f}}$; therefore the equation can be reduced to:

$$\sqrt{\frac{1}{f}} = -2 \cdot \log\left(\frac{K}{3.71 \cdot d_i}\right)$$ **Equation 4.22a**

The TNO report (TNO 1982) states that error in the computed value of $\sqrt{\frac{1}{f}}$ using this simplified formula "is never more than 4.6%" with the largest errors occurring on the smallest pipe diameters.

The compressibility factor of the gas can be found using the Nelson-Obert generalized compressibility chart by calculating the reduced pressure (the ratio of the pressure in the aperture to the critical pressure) and the reduced temperature (the ratio of the gas temperature and the critical temperature). According to the TNO report (TNO 1982) the pressure in the aperture is approximately 0.55 times the initial pressure in the pipe.

However, the results of reduced release rate calculations are relatively insensitive to changes in compressibility normally found in pipelines as illustrated by the following example. Assuming the pressures in typical natural gas pipelines range from 500 to 1,500 psi and the temperature ranges from 40 to 150°F (499.7 to 609.7°R), the reduced

temperature ranges from 1.5 to 1.8, given methane has a critical pressure of approximately 508 psi and a critical temperature of approximately 343°R. Entering the Nelson-Obert compressibility chart using the various combinations results in compressibility factors ranging from approximately 0.86 to 0.98. A series of plots of release rates (fraction of initial) versus time for a 36-inch diameter natural gas pipeline for compressibility factors 0.7, 0.8, 0.9 and 1.0 is shown in Figure 4.3.

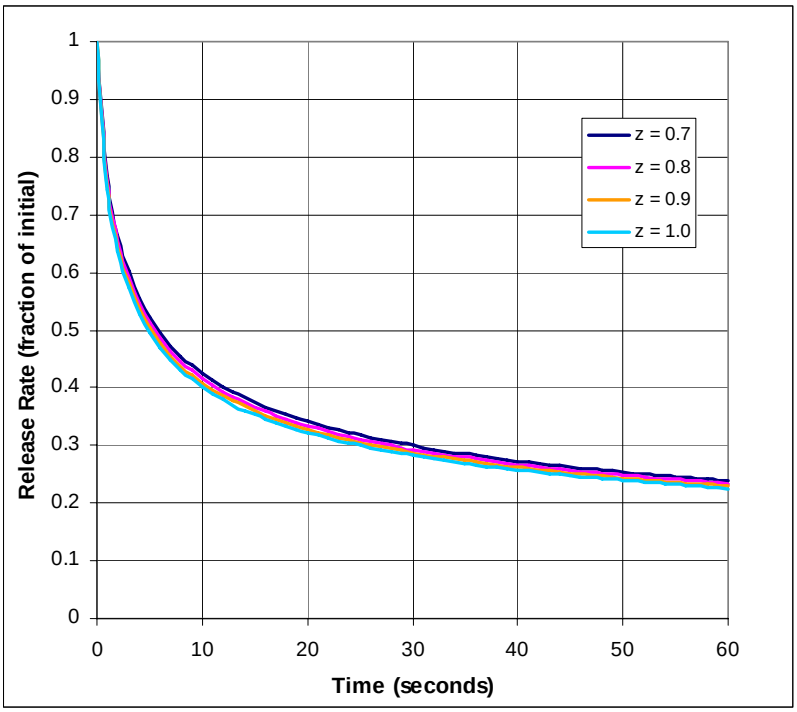

Figure 4.3 Release Rate versus Time for Various Compressibility Factors

While the area beneath the release rate versus time curve is related to the quantity released, and therefore the energy released, the more germane factor is the actual dose of thermal radiation received. A key consideration here is that the radiation dose equation is a nonlinear function of heat intensity and time. In addition, the original model assumed a somewhat delayed ignition, i.e., time of ignition is not equal zero on the curve. Nevertheless, since a simplified equation was the desired end result, a representative average release rate decay factor was determined by finding the constant value that corresponds to a comparable quantity released. This simplification is consistent with the methods used for determining other "constants" used in developing the original equation.

The original PIR formula derivation used a value of 0.33, which corresponds to the reduced release rate at ten seconds for a line having a diameter equal to the approximate weighted average of diameters of natural gas pipelines in service, as the representative average release rate decay factor, which results in a relative quantity release value of (0.33×30) 9.9. The actual area under the curve can be determined integrating Equation 4.20 from *t* equals 0 to *t* equals 30. This is represented by:

$$\int_0^{30} \left[1 + (0.75 \cdot t \cdot a)\right]^{-1/3} dt$$ **Equation 4.23**

where:

$$a = \left(\frac{f}{2 \cdot d}\right) \cdot \sqrt{\frac{z_u \cdot R \cdot T}{m}}$$

Integrating Equation 4.23 yields:

$$\frac{3}{2 \cdot a} \cdot \left[1 + a \cdot t\right]^{2/3} \Big|_0^{30}$$ **Equation 4.24**

Solving Equation 4.24 using the appropriate gas properties for methane and a diameter equal to the approximate weighted average of the diameters of natural gas lines in service results in a relative quantity release of 10.2. This value is approximately 2.9 percent higher than that calculated using the constant release rate decay factor over the same time period. The information used to calculate the weighted average diameter is presented in Table 4.12. The assumed representative diameter stated for each diameter range is conservatively assumed as the upper end of the range (42-inch diameter was chosen as the practical upper limit). The weighted average diameter was calculated as 22 inches.

Table 4.12 Weighted Average Diameter Calculation

NPS Range (in)	Approximate Length (miles)	Representative NPS (in)	Length × Diameter
< 4	27,000	4	108,000
4 to 10	69,000	10	690,000
10 to 20	84,000	20	1,680,000
20 to 28	45,000	28	1,260,000
> 28	63,000	42	2,646,000
Totals	288,000		6,384,000
Weighted Average Diameter = Sum of Length × Diameter / Sum of Length (6,384,000/288,000) =			22 inches

Plots of release rate versus time for several diameters, including the weighted average diameter, of natural gas pipelines (assumes pure methane) are presented in Figure 4.4. The release rate decay factor determined for methane is also shown as a solid horizontal line.

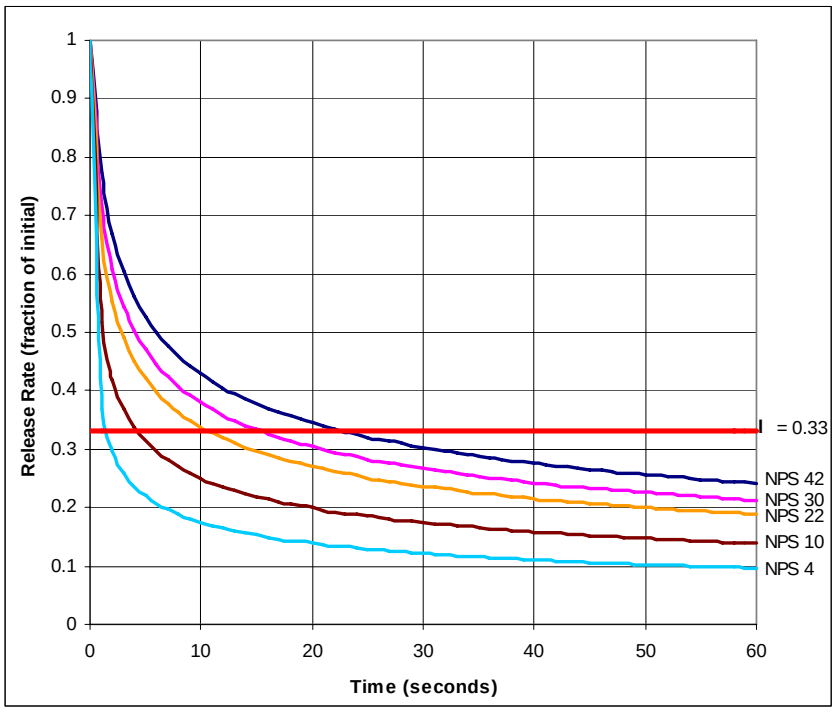

Figure 4.4 Release Rate versus Time for Methane

Following the procedure described above, a similar evaluation was conducted for rich natural gas, ethylene, hydrogen, and syngas. Based on the syngas discussion in Section 3.3, two different compositions of syngas were evaluated. Rich natural gas lines were assumed to have the same range of diameters and distribution as lean natural gas, thereby resulting in the same weighted average diameter. While a current range of hydrogen pipeline diameters is indicated by information in the NPMS, which indicates hydrogen is currently transported in smaller diameter pipelines, there are indications that industry is leaning towards larger, higher-pressure pipelines. Thus, for the purposes of determining an appropriate release rate decay factor for hydrogen pipelines, the weighted average diameter calculated for natural gas was also used. Similarly, since no information regarding diameter extremes for syngas and ethylene were available, it was assumed that the range of diameters indicated for the current population of hydrogen pipelines was appropriate and a straight average of the extreme NPS reported in the NPMS was used ([20+4]/2 = 12 inches) to determine an appropriate release rate decay factor for this product. Plots of release rate versus time for rich natural gas, ethylene, and hydrogen are presented in Figure 4.5, Figure 4.6, and Figure 4.7, respectively. Plots of release rate versus time for the two compositions of syngas evaluated are presented in Figure 4.8 and Figure 4.9.

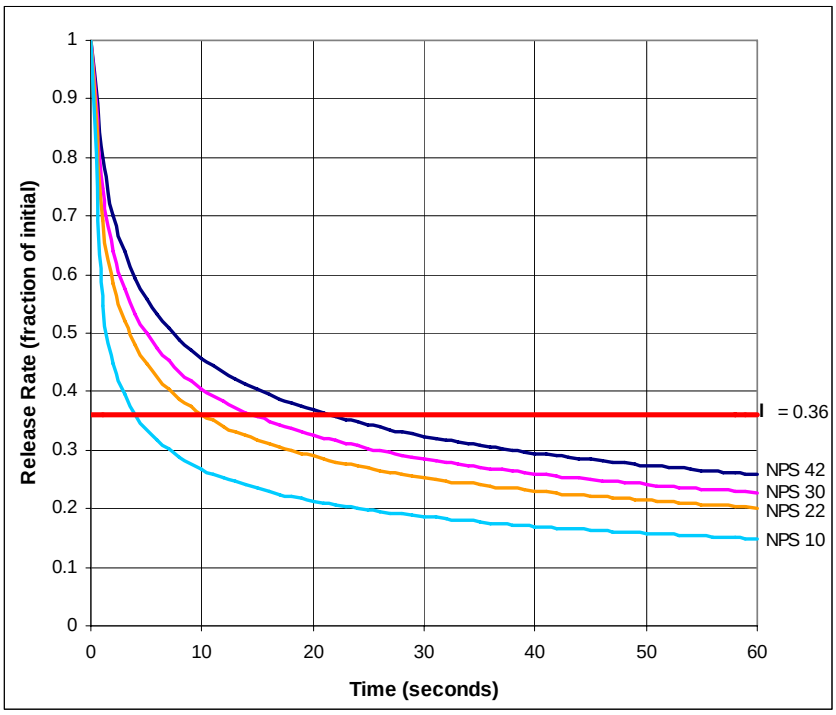

Figure 4.5 Release Rate versus Time for Rich Natural Gas

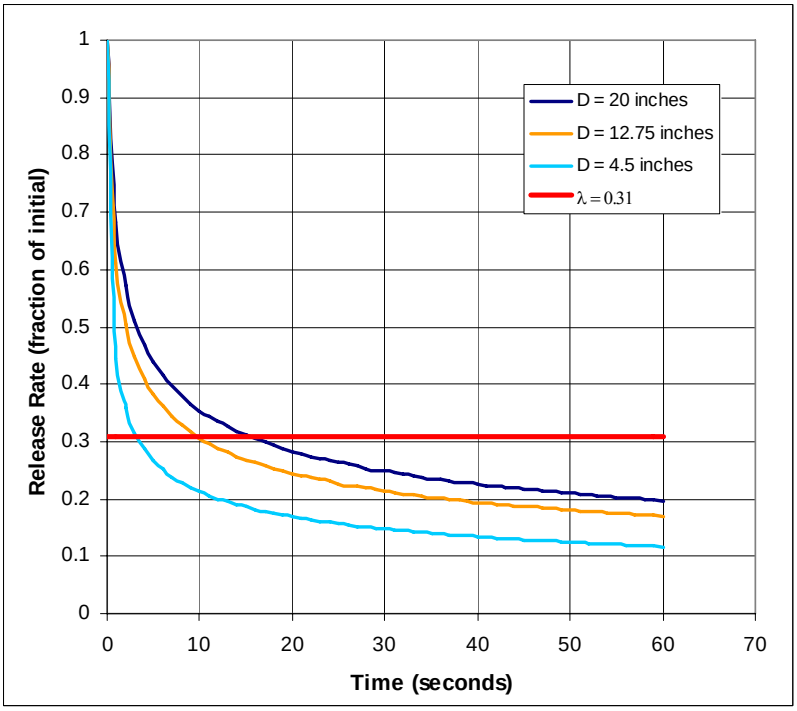

Figure 4.6 Release Rate versus Time for Ethylene

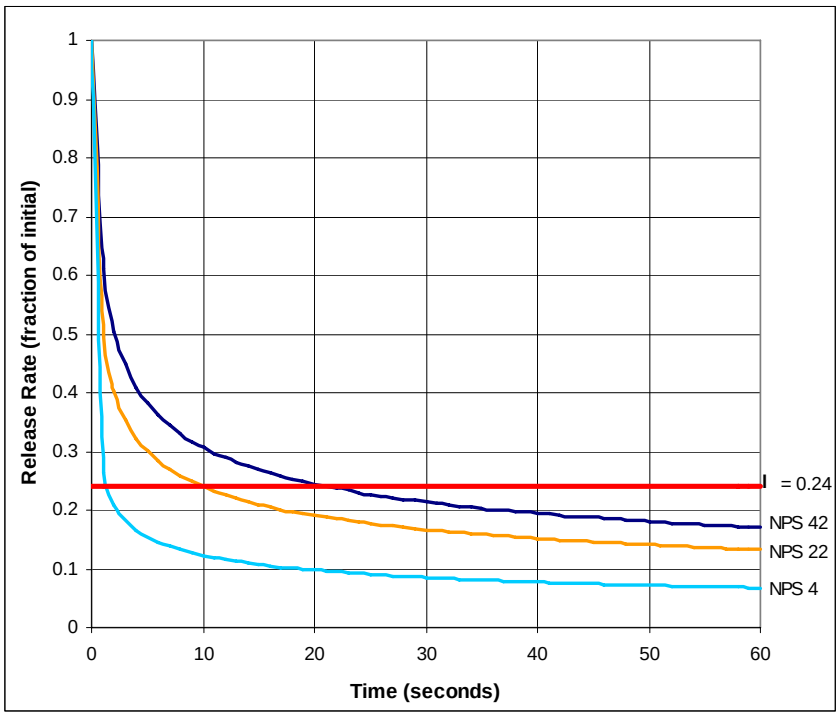

Figure 4.7 Release Rate versus Time for Hydrogen

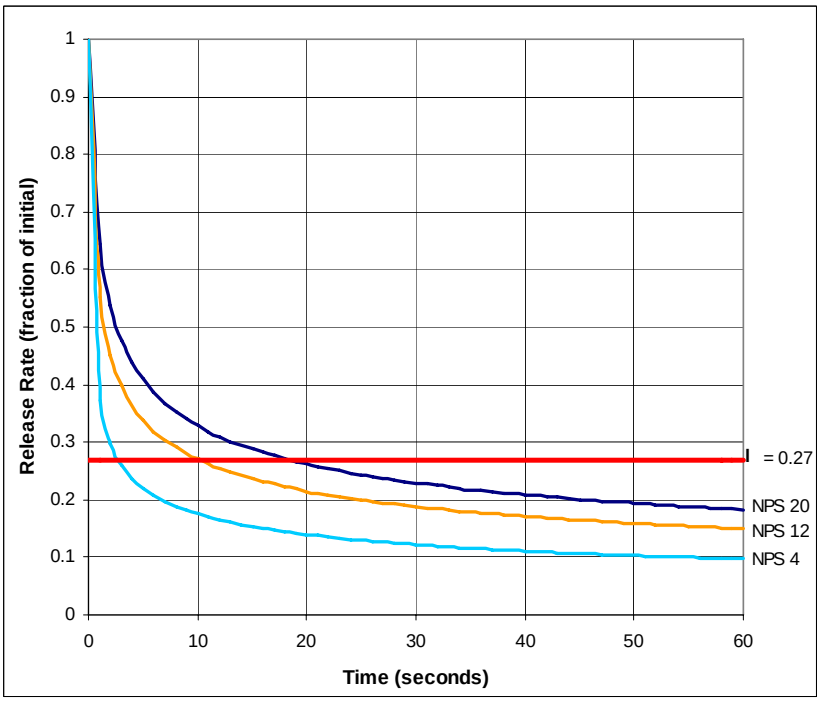

Figure 4.8 Release Rate Versus Time for Syngas
(Composition of 50 percent H_2 and 50 percent CO)

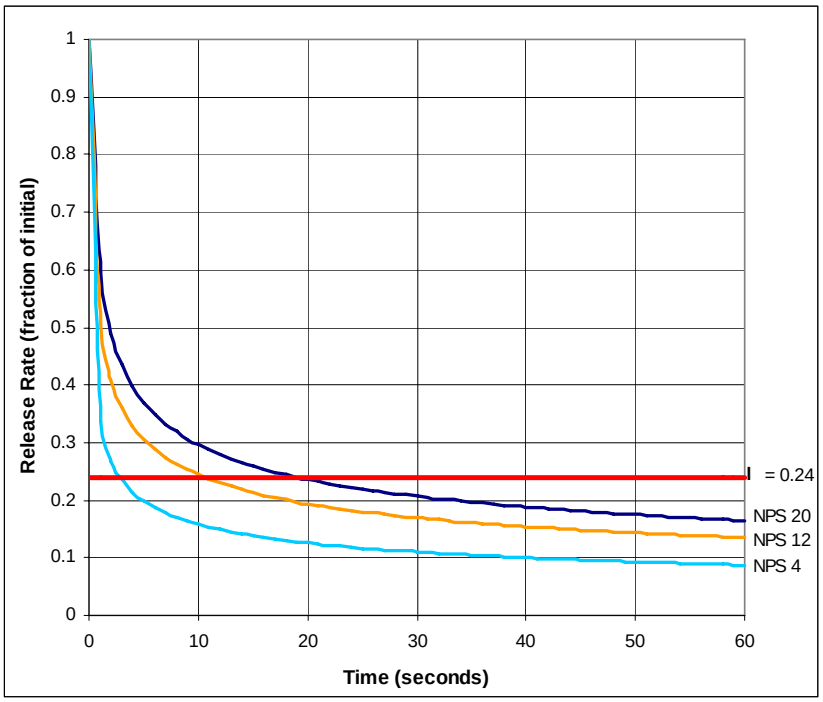

Figure 4.9 Release Rate Versus Time for Syngas
(Composition of 60 percent H_2, 30 percent CH_4 and 10 percent CO, representative of "coke" gas)

The release rate decay factor for each product shown in the above figures is presented in Table 4.13.

Table 4.13 Release Rate Decay Factors

Product	Release Rate Decay Factor
Ethylene	0.31
Hydrogen	0.24
Lean Natural Gas	0.33
Rich Natural Gas	0.36
Syngas (50% H_2/50% CO) (60% H_2/30% CH_4/10% CO)	 0.27 0.24

4.8 Potential Impact Radius Formula Derivation

Rearranging Equation 4.3 to solve for the effective gas release rate results in the form:

$$Q_{eff} = \frac{4 \cdot \pi \cdot r^2 \cdot I}{\mu \cdot X_g \cdot H_c} \qquad \textbf{Equation 4.25}$$

Setting Equation 4.4 equal to Equation 4.3 yields:

$$\frac{4 \cdot \pi \cdot r^2 \cdot I}{\mu \cdot X_g \cdot H_c} = 2 \cdot \lambda \cdot C_d \cdot \frac{\pi \cdot d^2}{4} \cdot p \cdot \frac{\varphi}{a_0} \qquad \textbf{Equation 4.26}$$

Rearranging Equation 4.10 and solving for *r*, gives:

$$r^2 = \frac{2 \cdot \lambda \cdot C_d \cdot \pi \cdot d^2 \cdot p \cdot \varphi \cdot \mu \cdot X_g \cdot H_c}{4 \cdot 4 \cdot I \cdot \pi \cdot a_o} = \frac{\mu \cdot X_g \cdot \lambda \cdot C_d \cdot \varphi \cdot H_c \cdot p \cdot d^2}{8 \cdot a_o \cdot I} \quad \text{or,}$$

$$r = \sqrt{\frac{\mu \cdot X_g \cdot \lambda \cdot C_d \cdot \varphi \cdot H_c \cdot p \cdot d^2}{8 \cdot a_o \cdot I}} \quad \textbf{Equation 4.27}$$

Care must be taken to ensure consistency of units. Thus, when working in Imperial units:

$$r = \sqrt{\frac{\mu \cdot X_g \cdot \lambda \cdot C_d \cdot \varphi \cdot \left(H_c \frac{BTU}{lbm}\right) \cdot \left(p \frac{lbf}{in^2}\right) \cdot \left(d^2 \cdot in^2\right)}{8 \cdot \left(a_o \frac{ft}{s}\right) \cdot \left(I \frac{BTU}{hr - ft^2}\right)}}$$

Since μ, X_g, λ, C_d, and φ are dimensionless, 1 hr = 3600 s, and 1 $lbf = 32.2 \frac{lbm - ft}{s^2}$, this results in:

$$r = \sqrt{\frac{\mu \cdot X_g \cdot \lambda \cdot C_d \cdot \varphi \cdot \left(H_c \frac{BTU}{lbm}\right) \cdot \left(p \frac{lbf}{in^2}\right) \cdot \left(32.2 \frac{lbm \cdot ft}{s^2 \cdot lbf}\right) \cdot \left(d^2 \cdot in^2\right)}{8 \cdot \left(a_o \frac{ft}{s}\right) \cdot \left(I \frac{BTU}{hr - ft^2}\right) \cdot \left(\frac{hr}{3600 \cdot s}\right)}}$$

Which simplifies to:

$$r = \sqrt{\frac{14490 \cdot \mu \cdot X_g \cdot \lambda \cdot C_d \cdot \varphi \cdot H_c \cdot p \cdot d^2}{a_o \cdot I}} \quad \textbf{Equation 4.28}$$

4.8.1 Gas Properties

The gas properties needed for the equations given above, and thus the final derivation of the Potential Impact Radius formula, include:

- molecular weight,
- specific heat ratio, and
- heat of combustion.

These values are presented in Table 4.14 for the four gases being considered. The properties for lean natural gas (pure methane) are also presented for comparison.

Table 4.14 Gas Properties

Product	Formula	Molecular Weight, m (lbm/lb-mole)	Specific Heat Ratio, γ	Heat of Combustion, H_c (BTU/lbm)
Ethylene	C_2H_4	28.05	1.22	20,275
Hydrogen	H_2	2.02	1.41	51,623
Lean Natural Gas	CH_4	16.04	1.31	21,495
Rich Natural Gas	Mixture	19.48	1.29	20,586
SynGas	50% H_2/50% CO	15	1.41	7,500
	60% H_2/30% CH_4/10% CO	8.83	1.40	20,188

4.8.2 Ethylene Calculations

The factors required to develop the Potential Impact Radius formula for ethylene using Equation 4.28 are summarized in Table 4.15.

Table 4.15 Factors for Ethylene

Factor	Value
Sonic velocity (ft/sec), a_0, = $\sqrt{\gamma RT/m}$	1055.3
Discharge coefficient (dimensionless), C_d	0.62
Heat of Combustion (Btu/lbm), H_c	20,275
Threshold Heat Flux (Btu/hr-ft^2), I_{th}	5,000
Molecular Weight (lbm/lb-mole), m	28.054
Gas Constant (ft-lbf/lb-mole-°R), R	1534
Gas Temperature (°R), T	518.4
Emissivity Factor (dimensionless), X_g	0.35
Specific Heat Ratio (dimensionless), γ	1.22
Release Rate Decay Factor (dimensionless), λ	0.31
Efficiency Factor (dimensionless), η	0.40
Flow Factor (dimensionless), $\varphi = \gamma \cdot \left(\frac{2}{\gamma+1}\right)^{\frac{\gamma+1}{2(\gamma-1)}}$	0.72

Substituting these factors into Equation 4.28 yields:

$$r = \sqrt{\frac{14490 \cdot 0.4 \cdot 0.35 \cdot 0.31 \cdot 0.62 \cdot 0.72 \cdot 20275 \cdot p \cdot d^2}{1055.3 \cdot 5000}} \quad \Rightarrow$$

$$r = \sqrt{1.08 \cdot p \cdot d^2} \quad \Rightarrow$$

$$r = 1.04 \cdot \sqrt{p \cdot d^2} \qquad \textbf{Equation 4.29}$$

4.8.3 Hydrogen Calculations

The factors required to develop the Potential Impact Radius formula for hydrogen are summarized in Table 4.16.

Table 4.16 Factors for Hydrogen

Factor	Value
Sonic velocity (ft/sec), a_0, = $\sqrt{\gamma RT/m}$	4251.6
Discharge coefficient (dimensionless), C_d	0.62
Heat of Combustion (Btu/lbm), H_c	51,623
Threshold Heat Flux (Btu/hr-ft^2), I_{th}	5,000
Molecular Weight (lbm/lb-mole), m	2.016
Gas Constant (ft-lbf/lb-mole-°R), R	1546
Gas Temperature (°R), T	518.4
Emissivity Factor (dimensionless), X_g	0.15
Specific Heat Ratio (dimensionless), γ	1.412
Release Rate Decay Factor (dimensionless), λ	0.24
Efficiency Factor (dimensionless), μ	0.35
Flow Factor (dimensionless), $\varphi = \gamma \cdot \left(\frac{2}{\gamma+1}\right)^{\frac{\gamma+1}{2(\gamma-1)}}$	0.82

Substituting these factors into Equation 4.28 yields:

$$r = \sqrt{\frac{14490 \cdot 0.35 \cdot 0.15 \cdot 0.24 \cdot 0.62 \cdot 0.82 \cdot 51623 \cdot p \cdot d^2}{4251.6 \cdot 5000}} \Rightarrow$$

$$r = \sqrt{0.22 \cdot p \cdot d^2} \Rightarrow$$

$$r = 0.47 \cdot \sqrt{p \cdot d^2} \qquad \textbf{Equation 4.30}$$

4.8.4 Rich Natural Gas Calculations

The factors required to develop the Potential Impact Radius formula for rich natural gas using Equation 4.28 are summarized in Table 4.17.

Table 4.17 Factors for Rich Natural Gas

Factor	Value
Sonic velocity (ft/sec), a_0, = $\sqrt{\gamma RT/m}$	1307.3
Discharge coefficient (dimensionless), C_d	0.62
Heat of Combustion (Btu/lbm), H_c	20,586
Threshold Heat Flux (Btu/hr-ft^2), I_{th}	5,000
Molecular Weight (lbm/lb-mole), m	19.48
Gas Constant (ft-lbf/lb-mole-°R), R	1546
Gas Temperature (°R), T	518.4
Emissivity Factor (dimensionless), X_g	0.2
Specific Heat Ratio (dimensionless), γ	1.29
Release Rate Decay Factor (dimensionless), λ	0.36
Efficiency Factor (dimensionless), μ	0.35
Flow Factor (dimensionless), φ = $\gamma \cdot \left(\frac{2}{\gamma+1}\right)^{\frac{\gamma+1}{2(\gamma-1)}}$	0.76

Substituting these factors into Equation 4.28 yields:

$$r = \sqrt{\frac{14490 \cdot 0.35 \cdot 0.2 \cdot 0.36 \cdot 0.62 \cdot 0.76 \cdot 20586 \cdot p \cdot d^2}{1307.3 \cdot 5000}} \Rightarrow$$

$$r = \sqrt{0.54 \cdot p \cdot d^2} \Rightarrow$$

$$r = 0.73 \cdot \sqrt{p \cdot d^2} \qquad \textbf{Equation 4.31}$$

4.8.5 Syngas Calculations

The factors required to develop a Potential Impact Radius formula for two example compositions of syngas using Equation 4.28 are summarized in Table 4.18.

Table 4.18 Factors for SynGas

Factor	Value	
	50% H_2/50% CO	60% H_2/30% CH_4/10% CO
Sonic velocity (ft/sec), a_0, = $\sqrt{\gamma RT/m}$	1557.5	2022.8
Discharge coefficient (dimensionless), C_d	0.62	0.62
Heat of Combustion (Btu/lbm), H_c	7,500	20,188
Threshold Heat Flux (Btu/hr-ft^2), I_{th}	5,000	5,000
Molecular Weight (lbm/lb-mole), m	15	8.83
Gas Constant (ft-lbf/lb-mole-°R), R	1546	1546
Gas Temperature (°R), T	518.4	518.4
Emissivity Factor (dimensionless), X_g	0.15	0.20
Specific Heat Ratio (dimensionless), γ	1.41	1.40
Release Rate Decay Factor (dimensionless), λ	0.27	0.24
Efficiency Factor (dimensionless), μ	0.35	0.35
Flow Factor (dimensionless), $\varphi = \gamma \cdot \left(\frac{2}{\gamma+1}\right)^{\frac{\gamma+1}{2(\gamma-1)}}$	0.82	0.81

Substituting these factors into Equation 4.28 yields:

$$r = \sqrt{\frac{14490 \cdot 0.35 \cdot 0.15 \cdot 0.27 \cdot 0.62 \cdot 0.82 \cdot 7500 \cdot p \cdot d^2}{1557.5 \cdot 5000}} \Rightarrow$$

$$r = \sqrt{0.10 \cdot p \cdot d^2} \Rightarrow$$

$$r = 0.32 \cdot \sqrt{p \cdot d^2} \quad \text{(50\% } H_2\text{/50\% CO)} \qquad \textbf{Equation 4.32}$$

$$r = \sqrt{\frac{14490 \cdot 0.35 \cdot 0.20 \cdot 0.24 \cdot 0.62 \cdot 0.81 \cdot 20188 \cdot p \cdot d^2}{2022.8 \cdot 5000}} \Rightarrow$$

$$r = \sqrt{0.244 \cdot p \cdot d^2} \Rightarrow$$

$$r = 0.49 \cdot \sqrt{p \cdot d^2} \quad \text{(60\% } H_2\text{/30\% } CH_4\text{/10\% CO)} \qquad \textbf{Equation 4.33}$$

While it is evident that application of Equation 4.32 would result in a smaller radius of impact than would be obtained using Equation 4.30 (pure hydrogen), the opposite is true if Equation 4.33 is used. Based on this information, it is recommended that Equation 4.32 be utilized for syngas, provided the composition contains no more than 30 percent methane. If this is not true for the composition being

evaluated, the formula for methane ($r = 0.69 \cdot \sqrt{p \cdot d^2}$) should be used. As an alternative, specific gas compositions can be analyzed and a composition specific formula developed using an emissivity factor of 0.2 and an efficiency factor of 0.35.

4.9 Mixed Gas Methodology

The derivation of a PIR formula for a mixed gas is identical to the process discussed above; however, appropriate values for several of the required parameters must be determined either by review of the information provided in this report or obtained elsewhere (emissivity factor, efficiency factor), or through calculation (molecular weight, specific heat ratio, heat of combustion, release rate decay factor, etc.).

A value of 0.25 for the emissivity factor (based on data for ethane and propane) is a reasonable upper bound if it is assumed that mixed gas will typically contain only more common naturally occurring substances (e.g., paraffinitic hydrocarbons, carbon monoxide, carbon dioxide, hydrogen, etc.).

Also, if it is assumed that the efficiency factor for mixed gas is comparable to that of rich natural gas or syngas since the major components of these gases are these same naturally occurring substances, then the appropriate value would be 0.35.

The molecular weight of mixed gas can be estimated using the following general formula:

$$m_{mix} = F_x \cdot m_x + F_y \cdot m_y + F_z \cdot m_z + \ldots \qquad \textbf{Equation 4.34}$$

where:

F_x = fraction of substance *x*;

F_y = fraction of substance *y*;

F_z = fraction of substance *z*;

m_x = molecular weight of substance *x*;

m_y = molecular weight of substance *y*; and

m_z = molecular weight of substance *z*.

Similarly, the heat of combustion of mixed gas can be estimated using the following general formula:

$$H_{C\,mix} = \frac{F_x \cdot m_x \cdot H_{Cx} + F_y \cdot m_y \cdot H_{Cy} + F_z \cdot m_z \cdot H_{Cz} + \ldots}{m_{mix}} \qquad \textbf{Equation 4.35}$$

where:

H_{Cx} = heat of combustion of substance *x*;

H_{Cy} = heat of combustion of substance *y*; and

H_{Cz} = heat of combustion of substance *z*.

Lastly, the specific heat ratio weight of mixed gas can be approximated using the following general formula:

$$\gamma_{mix} = F_x \cdot \gamma_x + F_y \cdot \gamma_y + F_z \cdot \gamma_z + \ldots \qquad \textbf{Equation 4.36}$$

where:

γ_x = specific heat ratio of substance *x*;

γ_y = specific heat ratio of substance *y*; and

γ_z = specific heat ratio of substance *z*.

The remaining parameters can then be calculated using Equations 4.18a, 4.18b, 4.20, 4.21, and 4.22a. The final PIR is then calculated using Equation 4.28.

4.9.1 Example of Mixed Gas Calculations

The following example demonstrates the calculation process for determining the PIR for mixed gas. The composition used (see Table 4.19) is typical of landfill gas. This example is for an NPS 16 pipeline operating at 100 psi.

Table 4.19 Mixed Gas Properties and Composition

Compound	Molecular Weight (lbm/lb-mole)	Specific Heat Ratio	Heat of Combustion (Btu/lbm)	Composition (%)
Methane	16.04	1.31	21,495	55.0
Nitrogen	28.02	1.40	0	10.0
Carbon Dioxide	44.01	1.30	0	35.0

Substituting the appropriate values from Table 4.19 into Equations 4.34, 4.35 and 4.36 to calculate the approximate molecular weight, specific heat ratio and heat of combustion of the mixture gives:

$$m_{mix} = 0.55 \cdot 16.04 + 0.1 \cdot 28.02 + 0.35 \cdot 44.01 = 27.03 \cdot lbm / lb - mole \text{ ;}$$

$$H_{C\,mix} = \frac{0.55 \cdot 16.04 \cdot 21495 + 0.1 \cdot 28.02 \cdot 0 + 0.35 \cdot 44.01 \cdot 0}{27.03} = 7{,}015 \cdot Btu / lbm \text{ ; and}$$

$$\gamma_{mix} = 0.55 \cdot 1.31 + 0.1 \cdot 1.40 + 0.35 \cdot 1.30 = 1.32 \text{ .}$$

Next, determine the flow factor of the mixed gas by substituting the specific heat ratio into Equation 4.18a:

$$\varphi = 1.32 \cdot \left(\frac{2}{1.32 + 1} \right)^{\frac{1.32+1}{2 \cdot (1.32-1)}} = 0.77 \text{ .}$$

The sonic velocity is calculated using Equation 4.18b. The universal gas constant, *R*, is normally given as 1,546 ft-lb/lb-mole °F. For this example, the gas temperature is assumed to be 59°F (518.4°R).

$$a_0 = \sqrt{\frac{1.32 \cdot 1546 \cdot 518.4 \cdot 32.2}{27.03}} = 1{,}122.6 \cdot \ ft/s \ .$$

[Note: The value 32.2 is the conversion from pound (mass) to pound (force), (*1 lbf = 32.2 lbm ft/s*^{2}).]

To determine the appropriate release rate decay factor, first calculate the friction factor using Equation 4.22a:

$$\sqrt{\frac{1}{f}} = -2 \cdot \log\left(\frac{0.00063}{3.71 \cdot 16}\right) = 9.95$$

Squaring both sides and inverting results in $f = 0.0101$. Assuming a compressibility factor of 1.0 (as shown in Section 4.7, moderate variations in the compressibility factor do not have significant impacts on release rate) and substituting the appropriate values (recall that ten seconds was taken as the appropriate time for establishment of the assumed radiation conditions) into Equation 4.21 gives:

$$t_r = 10 \cdot \left(\frac{0.0101}{2 \cdot 16/12}\right) \cdot \sqrt{\frac{1.0 \cdot 1546 \cdot 518.4 \cdot 32.2}{27.03}} = 37.02$$

[Note: For consistency of units, the diameter, *d*, must be in feet, hence the factor of 12 in the denominator above.]

Substituting this value into Equation 4.20 yields a reduced release rate of:

$$m_r = (1 + 0.75 \cdot 37.02)^{-1/3} = 0.33$$

This reduced release rate is the release rate decay factor.

Finally, substituting the appropriate values for all parameters in Equation 4.28 gives a PIR formula of:

$$r = \sqrt{\frac{14490 \cdot 0.35 \cdot 0.25 \cdot 0.33 \cdot 0.8 \cdot 0.77 \cdot 7015 \cdot p \cdot d^2}{1122.6 \cdot 5000}} \quad \Rightarrow$$

$$r = \sqrt{0.32 \cdot p \cdot d^2} \quad \Rightarrow$$

$$r = 0.57 \cdot \sqrt{p \cdot d^2}$$

Note that since methane is the only flammable gas in this mixture, use of the emissivity factor of methane (0.20) would be appropriate. Using the value of 0.25 recommended above for mixed gas results in a final PIR that is approximately 12 percent more conservative than that which would be calculated using the lower value.

5 Model Validation

Pipeline incident report listings available from the U.S. National Transportation Safety Board and Canada's Transportation Safety Board were reviewed in an attempt to locate data related to actual releases for the products of interest in this report to allow evaluations of the validity of the PIR formulae developed herein (Equations 4.29 through 4.33). However, no data was available and therefore, the formulae developed could not be validated.

This page intentionally left blank

6 Commentary on Recommended Model Factors

The discussion provided in Section 4, and Appendix A, indicates that some of the factors associated with the fire hazard model — namely, the release rate decay, and the emissivity and efficiency factors, presented in the development of the original model as product-specific constants — are in fact variables that depend to some extent on the physical and operational characteristics of the pipeline, the scale of the fire and the prevailing weather conditions. For example, the release rate decay is shown to be influenced by the diameter of the pipeline. The determination of the sustained release rate that should be used in the fire model (as obtained by multiplying the assumed rate decay factor by the peak initial release rate) is clearly dependent upon the assumed time delay between pipeline rupture and product ignition. The emissivity factor is reported to be influenced by the jet discharge velocity and the so-called flame residence time, which is a complex function of the initial jet diameter and discharge velocity, and the overall size of the fire. The efficiency factor is shown to be influenced by the size, shape, and opacity of the flame, the moisture content in the atmosphere, and the fire view distance.

In developing the original fire hazard model, these factors were treated as constants for simplicity of derivation and clarity of presentation, and because the effects of variations due to the above listed factors were assumed to be secondary. The original C-FER fire hazard model was put forward as a simplified steady-state approximation to a complex transient phenomenon that, for situations involving lean natural gas, provides reasonable estimates of the hazard zone dimensions as demonstrated by comparisons between predicted damage and the damage extent resulting from real pipeline failure incidents.

It is acknowledged that a more refined treatment of these model factors has the potential to improve the accuracy of the hazard zone estimation model. However, the accuracy achieved by treating these variables as constants is consistent with the simplified treatment of the fire itself — specifically the idealization of a large-scale transient fire as a steady state point source heat emitter. It is suggested that if the fire hazard model is to be refined by addressing some or all of the variabilities inherent in the release rate decay, and emissivity and efficiency factors, it should be carried out in combination with a comparably more sophisticated treatment of the flame. In this context, consideration should be given to replacing the single point source heat emitter model with a multiple point source emitter model or perhaps even a solid flame model. Consideration should also be given to the transient nature of the fire and its effect on the dose of thermal radiation received by damage receptors within the assumed reference exposure period.

In addition, further refinement of this thermal radiation model for use in characterizing the hazard zones for predominantly non-luminous flames, such as hydrogen (and potentially syngas), is inappropriate. Due to the rapid attenuation of thermal radiation intensity with distance for these flames, the dominant hazard may be the potential for direct exposure to flame, rather than exposure to a prescribed radiant heat intensity (see Appendix A and Section 4.5.7).

It is cautioned that while the current model, as a package, produces reasonable hazard zone estimates (as demonstrated for lean natural gas), selective refinement of individual model components may not improve the model accuracy, due to the complexities involved. Consider the following: if the simple model contains two factors with systematic biases that compensate for one another, then refined treatment of only one of the two factors will not in itself yield an improved model. In fact, the resulting model will be less accurate. To avoid this situation, all aspects of the model should be refined to a comparable degree.

Model refinement along the lines described above is clearly outside the current work scope, which is to address significant product-dependent changes that fundamentally alter the factors in the original fire hazard model. However, to provide added confidence in the continued use of the current model, consideration should be given to a follow-on study in which the issues raised can be fully explored.

7 Conclusions

Following the procedures discussed above and consistent with development of the PIR formula given in 49 CFR 192, Subpart O, a single "generic" PIR formula was developed for each of the following products:

- ethylene,
- hydrogen,
- rich natural gas, and
- syngas.

In addition, a more general methodology was presented that can be used to determine the PIR of other flammable gas mixtures (see Section 4.9). Based on the stated objective of developing PIR formulae consistent with that given in 49 CFR 192, the resulting formulae, as well as the original PIR formula for lean natural gas, are summarized in Table 7.1.

Table 7.1 Summary of Potential Impact Radius Formulae

Product	PIR Formula
Ethylene	$r = 1.04 \cdot \sqrt{p \cdot d^2}$
Hydrogen	$r = 0.47 \cdot \sqrt{p \cdot d^2}$
Natural Gas (Lean)	$r = 0.69 \cdot \sqrt{p \cdot d^2}$
Natural Gas (Rich)	$r = 0.73 \cdot \sqrt{p \cdot d^2}$
Syngas	$r = 0.49 \cdot \sqrt{p \cdot d^2}$ Note 1
Note 1 See discussion in Section 4.8.5	

The recommended formula for rich gas is considered appropriate for natural gas compositions for which the gross heating value is greater than 1,100 Btu/cubic foot.

As discussed in Section 3.3, ethylene has a specific gravity of approximately 1 and therefore the possibility exists for the formation of a flammable vapor cloud that can drift downwind before encountering an ignition source resulting in a short-lived flash fire that would likely have a much broader impact than estimated by the PIR formula developed in this report. Thus, proper consideration to all possible hazard scenarios should be given when evaluated the potential impact from a rupture on an ethylene pipeline.

As discussed in Sections 4.5.3 and 4.5.7 hydrogen, and synthetic gases with a low hydrocarbon content, produce a nonluminous flame and are subject to rapid attenuation of thermal radiation with distance. This presents problems when trying to apply the fire model described in Section 4.3 to pipelines transporting products that produce nonluminous flames, since the original PIR formula derivation was based on the premise that the dominant hazard associated with flammable gas release

is thermal radiation, and that radiation intensity will remain significant well beyond the flame face. If radiation intensity away from the flame face is low due to rapid attenuation by the atmosphere, then the radiation hazard area will collapse to a size less than the actual flame length and become secondary to the hazard posed by direct exposure to the flame.

In recognition of the above issues, the derivation of PIR formulae for hydrogen and syngas were modified to predict a hazard zone radius comparable to the length of a possible directed jet. While this approach is considered reasonable, given the current state of the art, it is proposed as an interim solution until better information becomes available on the flame length and radiation characteristics of large-scale hydrogen fires.

8 References

Atallah, S. and S.K. Saxena. 1995. *Natural Gas Jet Flames*. Topical Report prepared for the Gas Research Institute. GRI-97/0123, August.

Bagster, D.G. and R.M Pitblado. 1989. *Thermal Hazards in the Process Industry*. Chemical Engineering Progress, July, pp. 69-75.

Becker, H.A., and D. Liang. 1982. *Total Emission of Soot and Thermal Radiation by Free Turbulent Diffusion Flames*. Combustion and Flame 44, pp. 305 – 318.

Bilo, M. and P.R. Kinsman, 1997, *Thermal Radiation Criteria Used in Pipeline Risk Assessment*, Pipes & Pipelines International, November-December, pp. 17-25.

Brzustowski, T.A., S.R. Gollahalli, M.P. Gupta, M. Kaptein, H.F. Sullivan. 1975. *Radiant Heating from Flares*. An ASME Publication, April.

Chamberlain, G.A. 1987. *Developments in Design Methods for Predicting Thermal Radiation from Flares*. Chemical Engineering Research and Design, Volume 65, July.

Cook, D.K., M. Fairweather, J. Hammonds, D.J. Hughes. 1987a. *Size and Radiative Characteristics of Natural Gas Flares. Part I – Field Scale Experiments*. Chemical Engineering Research and Design, Volume 65, July.

Cook, D.K., M. Fairweather, J. Hammonds D.J. Hughes. 1987b. *Size and Radiative Characteristics of Natural Gas Flares. Part II – Empirical Model*. Chemical Engineering Research and Design, Volume 65, July.

Eisenberg, N.A., C.J. Lynch, and R.J. Breeding, 1975, *Vulnerability Model: A Simulation System for Assessing Damage Resulting from Marine Spills*, Environmental Control, Report CG-D-136-75.

Hymes, I., 1983, *The Physiological and Pathological Effects of Thermal Radiation*, Systems Reliability Directorate, Report SRD, R275.

Schefer, R., B. Houf, B. Bourne, and J. Colton. 2004. *Measurements to Characterize the Thermal and Radiation Properties of an Open-flame Hydrogen Plume*. Presented at the 15th Annual Hydrogen Conference and Hydrogen Expo USA. April.

Stephens, M.J. 2000. *A Model for Sizing High Consequence Areas Associated with Natural Gas Pipelines*. Topical Report prepared for the Gas Research Institute. GRI-00/0189, October.

TNO, 1982, *Safety Report on the Transportation of Natural Gas and LPG by Underground Pipeline in the Netherlands*, Ref. No. 82-04180, File No. 8727-50960, November 29.

Zabetakis, M.G. and D.S. Burgess. 1961. *Research on the Hazards Associated with the Production and Handling of Liquid Hydrogen*. TN23.U7 No. 5707.

This page intentionally left blank

APPENDIX A

Product Specific Emissivity and Efficiency Factors for Use in the C-FER Fire Model

This page intentionally left blank

C-FER Technologies

200 Karl Clark Road
Edmonton, Alberta
Canada T6N 1H2
Tel 780.450.3300
Fax 780.450.3700
www.cfertech.com

Final Report

Product Specific Emissivity and Efficiency Factors for Use in the C-FER Fire Model

Prepared by
Mark Stephens, MSc, PEng

Reviewed by
Qishi Chen, PhD, PEng

June 2005
L136

PROJECT TEAM

Product Specific Emissivity and Efficiency Factors for Use in the C-FER Fire Model	C-FER Project: L136
Name	**Responsibility**
Mark Stephens, MSc, PEng	All aspects

REVISION HISTORY

Product Specific Emissivity and Efficiency Factors for Use in the C-FER Fire Model		C-FER Project: L136			
Revision	**Date**	**Description**	**Prepared**	**Reviewed**	**Approved**
1	17 November, 2004	Draft	Mark Stephens	Qishi Chen	---
2	24 January, 2005	Revised Draft	Mark Stephens	Qishi Chen	---
3	18 February, 2005	Revised Draft	Mark Stephens	Qishi Chen	---
4	6 June, 2005	Final	Mark Stephens	Qishi Chen	Tom Zimmerman

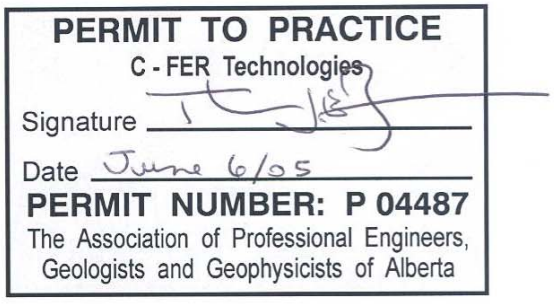

TABLE OF CONTENTS

NOTICE

1. This Report was prepared as an account of work conducted at C-FER Technologies on behalf of Michael Baker Jr., Inc. ("Baker"). All reasonable efforts were made to ensure that the work conforms to accepted scientific, engineering and environmental practices, but C-FER makes no other representation and gives no other warranty with respect to the reliability, accuracy, validity or fitness of the information, analysis and conclusions contained in this Report. Any and all implied or statutory warranties of merchantability or fitness for any purpose are expressly excluded. Any use or interpretation of the information, analysis or conclusions contained in this Report is at Baker's own risk. Reference herein to any specified commercial product, process or service by trade name, trademark, manufacturer or otherwise does not constitute or imply an endorsement or recommendation by C-FER.

2. Pursuant to the terms of the Subconsultant Agreement for Professional Services entered into the 1st day of September, 2004, any confidential and proprietary information contained in this Report is owned solely by Baker. C-FER confirms that Baker is entitled to make copies of this Report and to distribute copies of this report as Baker may require, but all such copies shall be copies of the entire Report. Baker shall not make copies of any extracts of this Report without the prior written consent of C-FER.

3.

LIST OF FIGURES AND TABLES

Figures

Tables

A.1 INTRODUCTION

The simple point source thermal radiation model developed by C-FER (Stephens 2000) for estimating heat intensity as a function of the distance from the point of pipeline failure to the location of interest is

$$I = \frac{\eta X_g Q_{eff} H_c}{4\pi r^2} \qquad [A.1]$$

where Q_{eff} = effective sustained release rate;
H_c = heat of combustion (a product property);
X_g = emissivity factor;
η = efficiency factor; and
r = radial distance from the point of failure to the location of interest.

The effective sustained release rate depends on the pipeline diameter and operating pressure and the properties of the product being transported. The initial release rate for a given product can be calculated directly using the release rate formula given in the original C-FER study. The effective sustained release rate, however, must be estimated from the initial release rate using a rate decay factor that is product dependent. In the original model, this factor was given as a constant (applicable to lean natural gas) but no guidance was provided on how to estimate the rate decay factor for other products. Rate decay factors appropriate for other product types have being developed as a separate task by Michael Baker Jr., Inc. (Baker). This document focuses on the effects of product type on the emissivity factor and the efficiency factor, which respectively relate to the magnitude of thermal radiation released by the fire and the amount of thermal radiation received by targets at a distance. Where required, use is made of the product specific release rate decay factors developed by Baker.

A.2 EMISSIVITY FACTOR

The emissivity factor in Equation [A.1] acknowledges that only a fraction of the heat energy theoretically released by combustion is dissipated through radiation. In general, the fraction of combustion energy that is radiated will depend on the efficiency of the combustion process, the tendency for the resulting flame to produce soot and the magnitude of heat lost by convection to the entrained air. The emissivity factor, also referred to in the literature as the 'radiant fraction', is product dependent. However, the discharge velocity and overall size of the fire can also have a significantly influence on the fraction of heat radiated. Discharge velocity is important because an increasing velocity is associated with a progressive increase in the degree of air-fuel mixing, which increases the proportion of heat lost to convection (Brzustowski et al 1975, Chamberlain 1987). The size of the fire is important because larger fires are associated with longer flame residence times and an increased residence time increases the fraction of heat that can be radiated (Becker and Liang 1982, Schefer et al. 2004).

Estimates of the radiant fraction reported in the literature are predominantly associated with small flares discharging at relatively low speeds (i.e. jets with velocities well below the sonic velocity). These values are generally assumed to provide reasonable estimates of the fraction of the heat radiated during controlled gas flaring operations; however, they are potentially inappropriate for use in assessing the heat radiated by a fire resulting from pipeline rupture, which can produce a very large flame and typically involves gas discharge under very high speed (i.e. sonic) conditions.

The emissivity factor (or radiant fraction) to be used in the C-FER model for a given product is the value applicable to relatively low speed (i.e. subsonic) jets, which would commonly be employed in flaring system design. An adjustment to this reference emissivity value, to make it more applicable to the estimation of the radiant heat energy produced by sonic jets feeding large-scale fires, is incorporated in the radiation efficiency factor (see Section A.3).

A literature survey was carried out to compile estimates of the radiant fraction for a range of hydrocarbon and non-hydrocarbon fuel sources. As noted, most of the available information comes from small-scale fire tests. The small-scale test data is summarized in Table A.1. Note that many references cite estimates of the radiant fraction that are directly or indirectly attributable to the early experiments of Zabetakis and Burgess (1961); only data from original sources is included in the table. Note also that the tabulated values are in all cases the maximum or upper plateau values recorded during the tests. Where testing programs also involved high-speed jets, all researchers reported a significant reduction in the radiant fraction with increasing jet velocity. Lastly, note that the high emissivity level associated with ethylene is primarily attributed to the fact that this fuel produces substantial amounts of soot when burned, and flames with a higher soot content are generally associated with higher emissivity levels.

Some large-scale fire test data is available for releases involving natural gas. Work by Chamberlain (1987) and Cook et al. (1987a) indicates that the effective radiant fraction for natural gas flares falls in the range of 0.34 to 0.07 with both studies clearly demonstrating that the radiant fraction falls with jet velocity. Best-fit relationships developed from the test data by these researchers suggest that for

Efficiency Factor

jet velocities in the range typical of conventional flaring operations (i.e. velocities in the range of Mach 0.2 to 0.5), the effective radiant fraction is in the range of 0.3 to 0.2, and under sonic discharge conditions (i.e. velocities above Mach 1.0) the radiant fraction falls below 0.16. This finding is particularly important because, as previously noted, under typical operating conditions, pipeline ruptures will always be associated with sonic discharge conditions.

Commodity	Source 1	Source 2	Source 3	Source 4	Source 5	Source 6	Source 7
Hydrogen	0.17					0.10	0.13
Syngas*					0.14		
Methane	0.16	0.2		0.18	0.18		
Natural Gas	0.23						
Ethane				0.24			
Propane		0.35	0.25	0.27	0.24		
Ethylene	0.38			0.31	0.34		

Source
1. Zabetakis and Burgess 1961
2. Brzustowski et al. 1975
3. Markstein 1975
4.Becker and Liang 1982
5.Turns and Myhr 1991
6. Barlow 2000
7. Schefer et al. 2004

** mixture consisting of 43% hydrogen and 57% carbon monoxide by volume*

Table A.1 Consolidation of Small-scale Test Data on Fraction of Heat Radiated

Note that in interpreting the results given in Table A.1, for the purpose of developing representative estimates of the emissivity factors, where significant differences were noted for a given product, greater weight was placed on the more recent test data assuming newer test methods and experimental equipment produce more accurate results.

Suggested emissivity factors for products of interest, developed from the above information, are given in Table A.2.

Efficiency Factor

Commodity	Factor
Hydrogen	0.15
Syngas	0.15
Natural Gas (lean)	0.20
Natural Gas (rich)	0.20
Ethylene	0.35

Table A.2 Suggested Emissivity Factors

With regard to lean natural gas, it is noted that the emissivity factor of 0.2, cited in the original derivation of the C-FER model and retained here, may appear somewhat non-conservative in light of the upper bound emissivity levels reported by Chamberlain (1987) and Cook et al. (1987a); however, as previously noted, the emissivity factors are effectively adjusted downwards (through the efficiency factor) to reflect conditions appropriate to sonic discharge events involving large-scale fires (see Section A.3).

Note that for rich gas, it is assumed that the emissivity is comparable to that of lean gas because the fractions of ethane and propane involved in a rich gas mixture are not substantial and because the reference emissivity values of the major components of rich gas are similar.

A.3 EFFICIENCY FACTOR

A.3.1 Basic for the Efficiency Factor

The efficiency factor is intended to address a number of conservatisms inherent in the simplified form of the model originally developed to estimate radiation intensity as a function of distance from the fire source. Specifically, it accounts for the conservatism associated with ignoring the following:

- the effect of high speed jetting and fire size on the total radiant heat energy produced;
- the effect of flame opacity on the amount of radiant heat energy released from the flame;
- the effect of flame height on the effective radiation distance; and
- the effect of atmospheric absorption on the amount of radiant heat reaching targets.

To understand the basis for the radiation efficiency factor incorporated in the original model, it is necessary to consider a more refined point source radiation model that explicitly addresses the effects noted above.

Such a model, as adapted from a widely recognized flare radiation model developed by Cook et al. (1987b), takes the following form

$$I = Q_{eff}\, H_c\, X_g^*\, \tau\, F_p \qquad [A.2]$$

where Q_{eff} = effective sustained gas release rate (kg/s);
H_c = heat of combustion (J/kg);
X_g^* = effective emissivity factor, adjusted for discharge velocity and fire size;
τ = atmospheric transmissivity; and
F_p = point source view factor (/m^2).

The effective emissivity factor is given by

$$X_g^* = X_g\, C_{Xg} \qquad [A.3]$$

where X_g = emissivity factor under conventional flaring conditions (see Section A.2); and
C_{Xg} = emissivity adjustment factor.

The view factor is given by

$$F_p = A_{iso}\, F_{iso} + (1 - A_{iso})F_{dif} \qquad [A.4]$$

Efficiency Factor

where A_{iso} is an empirically derived constant that determines the relative applicability of isotropic versus diffuse emission assumptions. (Effectively, the flame is treated as a mixed mode radiation emitter with the relative importance of isotropic versus diffuse emission processes being determined experimentally.)

Isotropic emission assumes an optically thin flame that is effectively transparent to radiation in all directions. The associated view factor is

$$F_{iso} = \frac{1}{4\pi x^2} \qquad [A.5]$$

where x is the line of sight distance (in meters) from the centre of the flame to the point of interest.

Diffuse emission assumes the flame is completely opaque, radiating only from the surface envelope. The associated view factor is

$$F_{dif} = \frac{\cos\theta}{4\pi x^2} \qquad [A.6]$$

where θ is angle subtended by the normal to the flame locus at the point source and the line joining the point source to the target.

Large scale experiments with natural gas flames led Cook et al. to conclude that the best correlation between predicted and actual radiation levels in both the near and far field is achieved using a value of A_{iso} equal to 0.5.

If the flame is assumed to be vertically oriented, and if it is further idealized as a single point source emitter located at flame mid-height, the fire geometry is as shown in Figure A.1.

Efficiency Factor

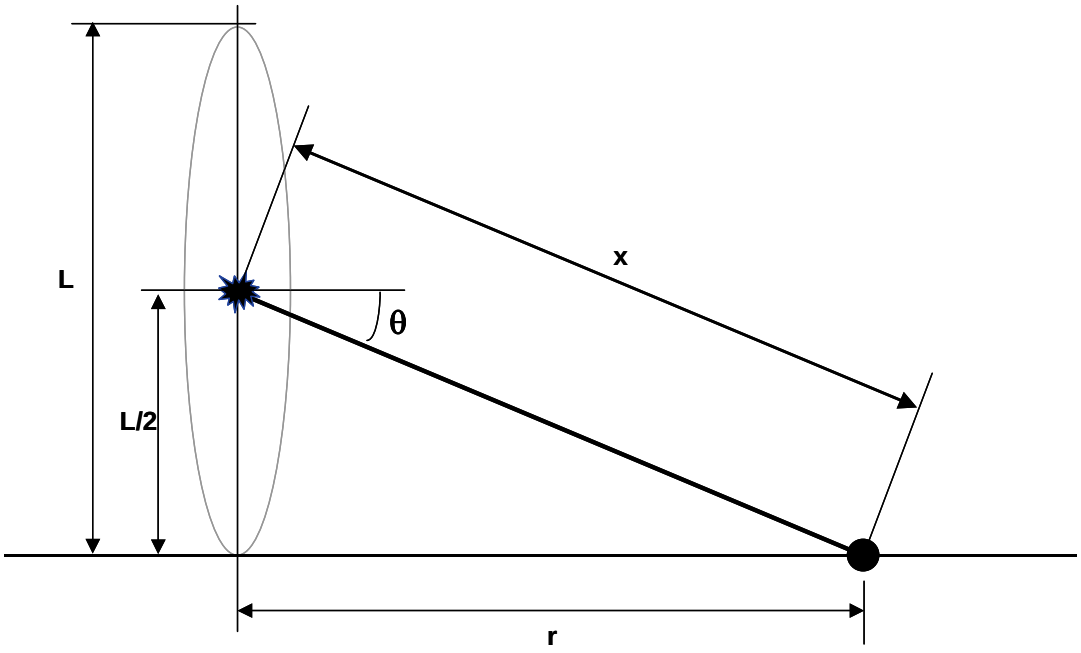

Figure A.1 Elevated Point Source Fire Model Geometry

From Figure A.1 it follows that the relationship between the line of sight distance, *x*, and the horizontal distance projection, *r*, is given by

$$x = \frac{r}{\cos\theta} \qquad [A.7]$$

where the view angle, θ, is given by

$$\theta = \arctan\left(\frac{L/2}{r}\right) \qquad [A.8]$$

Substituting Equations [A.3] through [A.7] into Equation [A.2], and expressing the distance in terms of the horizontal projection using Equation [A.7], the resulting point source radiation model is

$$I = \frac{X_g\, C_{Xg}\, \tau\, Q_{eff}\, H_c}{4\pi r^2} \cos^2\theta\left(0.5 + 0.5\cos\theta\right) \qquad [A.9]$$

Comparison of the radiation intensity model given by Equation [A.9] with the original C-FER point source model given by Equation [A.1] shows that the two are equivalent if the efficiency factor in the original model is equal to

Efficiency Factor

$$\eta = C_{Xg}\,\tau \cos^2\theta \left[0.5 + 0.5\cos\theta\right] \qquad \text{[A.10]}$$

To quantify the efficiency factor, estimates are required of the view angle, θ, the atmospheric transmissivity, τ, and the emissivity adjustment factor, C_{Xg}.

A.3.2 Elements of the Efficiency Factor

View Angle

To estimate the view angle, an estimate of the flame length is required. For large-scale hydrocarbon fires, the flame length can be estimated using the GRI flame length model (GRI 1995). This simple empirical model was developed through regression analysis of data from pipeline failure reports published by the Transportation Safety Board, the results of large-scale experiments on natural gas and LPG published in the literature and observations made during oil well fires. According to this model, the flame length (in meters) is given by

$$L = 0.0274\left(Q_{eff}\,H_c\right)^{0.352} \qquad \text{[A.11]}$$

For a given release scenario, Equation [A.11], in conjunction with Equations [A.8] and [A.9], can be used to estimate the view angle. Note that the interdependence of the parameters in these equations makes this an iterative calculation process. It also requires an estimate of the atmospheric transmissivity, τ, and the emissivity adjustment factor, C_{Xg}.

Atmospheric Transmissivity

A portion of the heat energy radiated from a fire is absorbed and scattered by the atmosphere causing a reduction in the radiation received by targets at some distance from the flame. The amount radiation lost to the atmosphere depends on the wavelength of the radiation, the amount of water vapour in the atmosphere and the distance traveled. For hydrocarbon fires, which radiate a significant proportion of their heat energy within the visible spectrum (i.e. for luminous flames), these radiation losses typically range between 10% and 40%.

Atmospheric transmissivity is a measure of the fraction of radiant energy reaching a target. Numerous models are available for estimating the transmissivity of the atmosphere to radiation from luminous flames. A widely cited formula is (Bagster and Pitblado 1989)

$$\tau = 2.02\,(P_w\,x)^{-0.09} \qquad \text{[A.12a]}$$

where P_w = partial pressure of water vapour in the atmosphere (Pa); and
x = line of sight distance (m).

Efficiency Factor

The partial pressure of water vapour is a function of air temperature and humidity level. It can be estimated from

$$P_w = RH\, P_w^0 = RH(610.7 \times 10^{[7.5T/(237.3+T)]}) \qquad \text{[A.12b]}$$

where P_w^0 = saturated vapour pressure of water in the atmosphere (Pa);
RH = relative humidity (fraction); and
T = air temperature (ºC).

When atmospheric transmissivity is to be estimated in a generic sense, it is common to assume an air temperature and relative humidity that is associated with a conservatively low estimate of the level of water vapour in the atmosphere, because a low water vapour content is associated with a higher transmissivity. If the air temperature is assumed to be 15ºC, consistent with the assumption made in developing the original C-FER fire model, and the relative humidity is assumed to be 40%, the atmospheric transmissivity versus line of sight distance is as shown in Figure A.2.

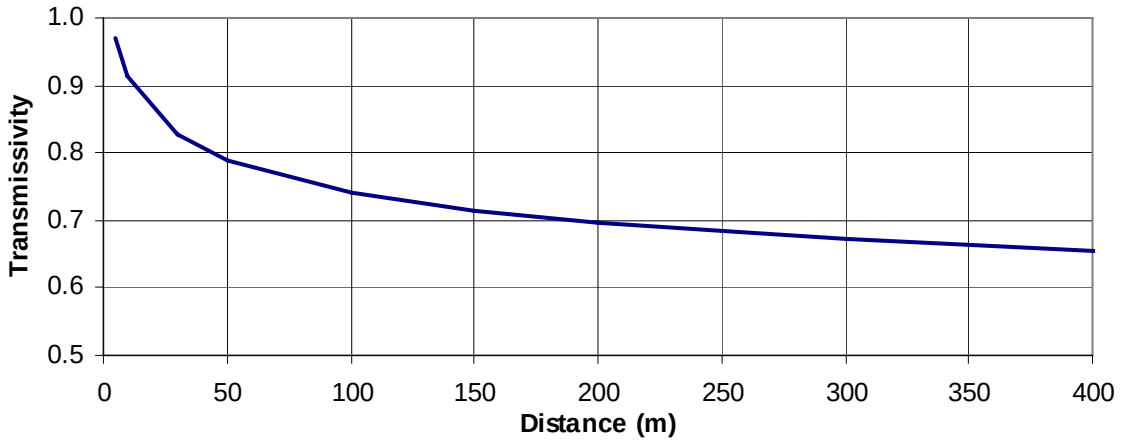

Figure A.2 Atmospheric Transmissivity for Hydrocarbon Flames

For products that produce fires that radiate primarily outside the visible spectrum (i.e. for nonluminous flames), the usual hydrocarbon fire transmissivity models are not applicable. Examples of products producing a largely invisible flame include: hydrogen, synthetic gases (i.e. syngas) for which the dominant constituents are hydrogen and carbon monoxide, and methanol.

Unfortunately, limited information is available on the transmissivity of nonluminous flames over significant distances. The only directly relevant information found in the literature is a hydrogen fire transmissivity formula developed over 40 years ago by Zabetakis and Burgess (1961). This model takes the form

$$\tau = e^{-0.0492\, w\, x} \qquad \text{[A.13a]}$$

Efficiency Factor

where w = water content of the atmosphere (% by weight); and
x = line of sight distance (m).

The water content by weight percent is given by

$$w = 6.2 \times 10^{-4} P_w \qquad \text{[A.13b]}$$

where P_w is given by Equation [A.12b].

If the assumptions for air temperature and humidity are the same as those made for hydrocarbon flames, the atmospheric transmissivity versus line of sight distance for hydrogen fires is as shown in Figure A.3. For comparison, the transmissivity function developed above for hydrocarbon flames is shown as well.

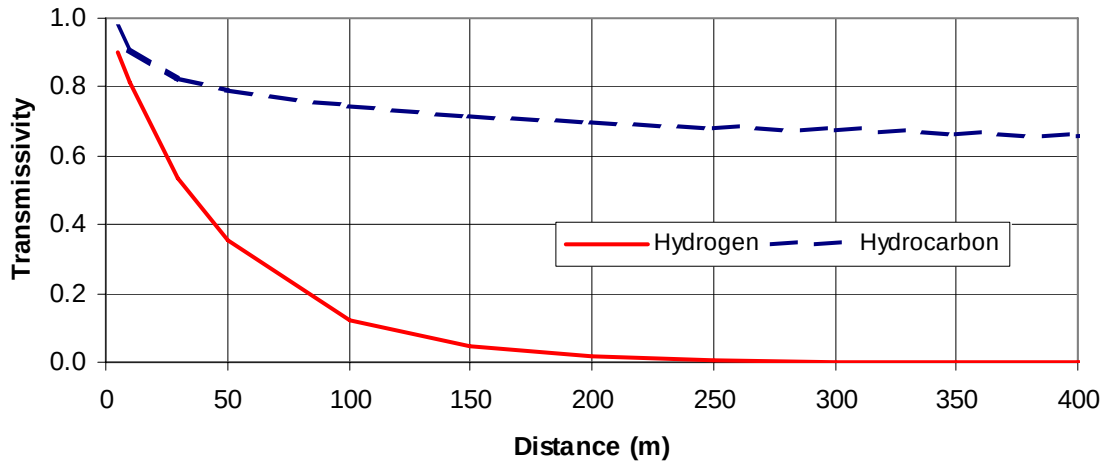

Figure A.3 Transmissivity Comparison between Hydrogen and Hydrocarbon Flames

The figure shows the transmissivity of the atmosphere to radiation from a nonluminous hydrogen flame falls much more rapidly with distance than does the transmissivity for a luminous hydrocarbon flame.

It is noted that the relationship developed by Zabetakis and Burgess was based on laboratory scale experiments and limited field-testing. The validity of this model for estimating transmissivity over significant distances is therefore not as well established as the model presented for luminous hydrocarbon flames. However, the trend indicated by the model is supported by a substantial body of anecdotal information, which indicates that the major concern with hydrogen fires is that they are difficult to see (i.e. the flame is nearly invisible) and that the rapid attenuation of radiation by the atmosphere makes it difficult for a person to gauge distance to the flame face. This anecdotal information suggests that the dominant hazard to people is inadvertent direct exposure to the flame rather than thermal radiation at a distance. This presents a significant problem when trying to characterize the hazard zone for products that produce nonluminous flames (see Section A.3.4.2).

Efficiency Factor

Emissivity Adjustment

As discussed in Section A.2, the emissivity factor that is to be used in the C-FER model (Equation [A.1]) is the commonly cited emissivity level (or radiant fraction) applicable to controlled gas flaring operations. Also as discussed, these emissivity levels are not considered directly applicable to large fires produced by gas jets discharging at high velocities. An adjustment is therefore considered appropriate when considering radiation from pipeline rupture fires, which can be very large and which are typically associated with sonic discharge conditions during the early stages of a release event.

Unfortunately, limited information is available on the emissivity of large–scale fires fed by sonic jets. The best information available pertains to natural gas. Large-scale flare test data reported by Chamberlain (1987) and Cook et al. (1987b) suggests that for jet velocities at, or above, the sonic velocity of natural gas, the measured emissivity of the flame is at least 25% to 50% lower than the emissivity measured at low velocities. In addition, best-fit relationships developed by these researchers indicate that at jet velocities at, or above, the sonic velocity, the actual emissivity is below 0.16. Based on this information an emissivity adjustment factor of C_{Xg} = 0.75 is considered appropriate for natural gas. This reduces the emissivity of natural gas from the assumed reference value of 0.2 to an effective value of 0.15, which compares favourably with the values given by the regression models developed by both Chamberlain (1987) and Cook et al. (1987) for sonic discharges involving large flames.

No comparable information is available for other products. However, as noted in Section A.2, small-scale test data indicates that all products of interest exhibit a reduction in emissivity with increased jetting velocity. In the absence of product-specific data, the emissivity adjustment factor adopted for natural gas is assumed to be applicable to all products of interest.

A.3.3 Validation of Efficiency Factor for Lean Natural Gas

Given the approach described in Section A.3.2, estimates of the radiation efficiency factor, consistent with the refined thermal radiation hazard model, can be developed for natural gas pipelines over a range of diameter-pressure combinations. Table A.3 summarizes the values obtained for lean natural gas as represented by the properties of methane.

The results given in Table A.3 show that the efficiency factor used in the development of the original model (i.e. η = 0.35) is conservative for small diameter, low-pressure pipelines and slightly non-conservative for large diameter, high-pressure lines. Given the range and central tendency of the tabulated estimates of the efficiency factor, the adopted reference value is shown to be a reasonable single valued approximation to the range of efficiency factors that apply to the natural gas pipeline population as a whole.

Efficiency Factor

Dia. d (in)	Press. p (psi)	Power Q_{eff} H_c (kJ/s)	Zone Radius* r (m)	Flame Height L (m)	View Angle (deg)	Sight Dist. x (m)	Atmos. Trans.	Emissivity Adjust. C_{Xg}	Efficiency Factor
6.625	500	2.71×10^6	23.2	57.3	51.0	36.9	0.812	0.75	0.197
12.75	750	1.51×10^7	70.5	105	36.6	87.9	0.751	0.75	0.327
24	1000	7.12×10^8	165	181	28.8	188	0.701	0.75	0.379
36	1250	2.00×10^8	283	261	24.8	311	0.670	0.75	0.395
42	1500	3.27×10^8	363	310	23.1	395	0.656	0.75	0.399
								Average→	**0.34**

Assumed lean gas properties (100% methane): M = 16.04 g/mol, γ = 1.306, H_c = 50,000 kJ/kg
*Hazard zone radius calculated assuming:
- heat intensity threshold = 15.77 kW/m2
- emissivity factor = 0.2
- release rate decay factor = 0.33

Table A.3 Radiation Efficiency Factors for Lean Natural Gas Pipelines

A.3.4 Efficiency Factor for other Products

A.3.4.1 Products Associated with Luminous Flames

Rich Gas

For a rich natural gas, the efficiency factor estimates obtained using the approach described in Section A.3.2, are summarized in Table A.4 for a representative range of diameter-pressure combinations.

The results show that the efficiency factor developed for lean natural gas (η = 0.35) is equally applicable to rich gas. This is because the chemical power associated with rupture failure (i.e. the product of Q_{eff} and H_c) is similar for both lean and rich gases and the emissivity or radiant fraction for both product mixtures is essentially the same.

Efficiency Factor

Dia. d (in)	**Press. p** (psi)	**Power** $Q_{eff}\ H_c$ (kJ/s)	**Zone Radius* r** (m)	**Flame Height** L (m)	**View Angle** θ (deg)	**Sight Dist.** x (m)	**Atmos. Trans.** τ	**Emissivity Adjust.** C_{Xg}	**Efficiency Factor** η
6.625	500	3.11×10^6	25.8	60.1	49.4	39.6	0.806	0.75	0.212
12.75	750	1.73×10^7	76.2	110	35.8	94.0	0.746	0.75	0.333
24	1000	8.16×10^8	177	190	28.2	201	0.697	0.75	0.382
36	1250	2.30×10^8	303	273	24.3	333	0.666	0.75	0.397
42	1500	3.75×10^8	389	325	22.7	422	0.652	0.75	0.400
								Average→	**0.35**

Assumed rich gas properties (80% methane, 15% ethane, 3% propane, 0.5% butane, 1.5% other) :
M = 19.48 g/mol, γ = 1.29, H_c = 47,886 kJ/kg
*Hazard zone radius calculated assuming:
- heat intensity threshold = 15.77 kW/m2
- emissivity factor = 0.2
- release rate decay factor = 0.36

Table A.4 Radiation Efficiency Factors for Rich Natural Gas Pipelines

Ethylene

For ethylene, the calculated efficiency factor estimates are summarized in Table A.5. The adopted diameter-pressure range differs from the range used for natural gas pipelines. A smaller diameter range was used because it is considered more representative of refined product pipelines.

The results suggest that an efficiency factor of 0.4 is more appropriate for this product.

Efficiency Factor

Dia. d (in)	**Press. p** (psi)	**Power** Q_{eff} H_c (kJ/s)	**Zone Radius*** r (m)	**Flame Height** L (m)	**View Angle** θ (deg)	**Sight Dist.** x (m)	**Atmos. Trans.** τ	**Emissivity Adjust.** C_{xg}	**Efficiency Factor** η
4.5	500	1.43×10^6	29.2	45.8	38.1	37.1	0.811	0.75	0.337
12.75	1000	2.30×10^7	131	122	24.9	144	0.718	0.75	0.422
20	1500	8.48×10^8	254	193	20.8	271	0.678	0.75	0.430
								Average→	**0.40**

Assumed ethylene properties: M = 28.05 g/mol, γ = 1.22, H_c = 47,162 kJ/kg

*Hazard zone radius calculated assuming:

- heat intensity threshold = 15.77 kW/m2
- emissivity factor = 0.35,
- release rate decay factor = 0.31

Table A.5 Radiation Efficiency Factors for Ethylene Pipelines

A.3.4.2 Products Associated with Nonluminous Flames

If it is assumed that the previously described atmospheric transmissivity relationship given by Zabatekis and Burgess for hydrogen flames (see Section A.3.2) is reasonable and applicable to nonluminous flames in general, the extremely rapid attenuation of thermal radiation with distance indicated by their model presents a problem when trying to apply the C-FER fire hazard model to pipelines transporting hydrogen and other products that produce nonluminous flames. The C-FER model was developed assuming that the dominant hazard is thermal radiation and that radiation intensity will remain significant well beyond the flame face. This is fundamental to the hazard zone radius estimation procedure. If radiation intensity away from the flame face is low, due to rapid attenuation by the atmosphere, then the radiation hazard area will collapse to a size significantly less than the flame length and become secondary to the hazard posed by direct exposure to the flame.

In an attempt to address the flame exposure hazard using the existing thermal radiation hazard model framework, it is suggested that until better information becomes available on the radiation characteristics of large-scale fires involving nonluminous flames, the hazard zone radius should be made to be comparable to the length of a possible directed jet. Unfortunately, this approach presents difficulties as well; a proven model for estimating the length of large-scale hydrogen flames is not yet available. As an interim approach, it is proposed that the efficiency factor for nonluminous flames should be chosen to ensure that the hazard zone radius obtained from the C-FER model is comparable to the flame length estimated using Equation [A.11], assuming that for a directed jet the mass flow feeding the flame is the discharge from a single end of the pipe (i.e. use 1/2 Q_{eff} in Equation [A.11]).

Efficiency Factor

The length of a directed jet, as calculated using Equation [A.11] with a reduced effective mass flow rate, is shown in comparison to the hazard zone radius given by the existing hazard zone model in Table A.6, for a range of hydrogen pipeline diameter-pressure combinations. Similar results are given for syngas pipelines in Table A.7. It is shown in both tables that the zone radius is comparable to the flame length if the value of the efficiency factor proposed in the original model is retained. Based on this rationale, it is proposed that the value of the efficiency factor originally proposed for natural gas should also be used for hydrogen and synthetic gas as well.

Diameter **d** (in)	**Pressure** **p** (psi)	**Total Power** $Q_{eff}\,H_c$ (kJ/s)	**Zone Radius*** ***r*** (m)	**Half Power** $\frac{1}{2}*Q_{eff}\,H_c$ (kJ/s)	**Directed Jet Length** ***L*** (m)
6.625	500	1.72×10^6	21.4	8.62×10^5	38.3
12.75	750	9.58×10^6	50.4	4.79×10^6	70.0
24	1000	4.53×10^7	110	2.26×10^7	121
36	1250	1.27×10^8	184	6.37×10^7	174
42	1500	2.08×10^8	235	1.04×10^8	207

Assumed hydrogen properties: M = 2.016 g/mol, γ = 1.412, H_c = 120,000 kJ/kg

*Zone radius calculated assuming:

- heat intensity threshold = 15.77 kW/m2
- efficiency factor = 0.35
- emissivity factor = 0.15,
- release rate decay factor = 0.24

Table A.6 Hazard Zone Radius Versus Directed Jet Length for Hydrogen Pipelines

Efficiency Factor

Diameter **d** (in)	**Pressure** **p** (psi)	**Total Power** $Q_{eff}\,H_c$ (kJ/s)	**Zone Radius*** ***r*** (m)	**Half Power** $\frac{1}{2}*Q_{eff}\,H_c$ (kJ/s)	**Directed Jet Length** ***L*** (m)
6.625	500	7.72×10^5	14.3	3.86×10^5	28.8
12.75	750	4.29×10^6	33.7	2.14×10^6	52.8
24	1000	2.03×10^7	73.2	1.01×10^7	91.1
36	1250	5.70×10^7	123	2.85×10^7	131
42	1500	9.30×10^7	157	4.65×10^7	156

Assumed syngas properties (50% hydrogen, 50% carbon monoxide):
M = 15 g/mol, γ = 1.41, H_c = 17,500 kJ/kg
*Zone radius calculated assuming:
- heat intensity threshold = 15.77 kW/m2
- efficiency factor = 0.35
- emissivity factor = 0.15,
- release rate decay factor = 0.27

Table A.7 Hazard Zone Radius Versus Directed Jet Length for Syngas Pipelines

A.3.5 Summary of Suggested Efficiency Factors

Suggested radiation efficiency factors for products of interest, developed as described above, are summarized in Table A.8.

Commodity	Factor
Hydrogen	0.35
Syngas	0.35
Natural Gas (lean)	0.35
Natural Gas (rich)	0.35
Ethylene	0.40

Table A.8 Suggested Efficiency Factors

A.4 REFERENCES

Bagster, D.G. and Pitblado, R.M. 1989. Thermal Hazards in the Process Industry. Chemical Engineering Progress, July 1989, pages 69 - 75.

Barlow, R.S. 2000. International Workshop on Measurement and Computation of Turbulent Nonpremixed Flames. Combustion Research Facility, Sandia National Laboratories.

Becker, H.A., Liang, D. 1982. Total Emission of Soot and Thermal Radiation by Free Turbulent Diffusion Flames. Combustion and Flame, 44 pages 305 – 318.

Brzustowski, T.A., Gollahalli, S.R., Gupta, M.P., Kaptein, M., Sullivan, H.F. 1975. Radiant Heating from Flares. An ASME Publication, April.

Chamberlain, G.A. 1987. Developments in Design Methods for Predicting Thermal Radiation from Flares. Chemical Engineering Research and Design, Volume 65, July.

Cook, D.K., Fairweather, M., Hammonds, J., Hughes, D.J. 1987a. Size and Radiative Characteristics of Natural Gas Flares. Part I – Field Scale Experiments. Chemical Engineering Research and Design, Volume 65, July.

Cook, D.K., Fairweather, M., Hammonds, J., Hughes, D.J. 1987b. Size and Radiative Characteristics of Natural Gas Flares. Part II – Empirical Model. Chemical Engineering Research and Design, Volume 65, July.

GRI 1995. Natural Gas Jet Flames. Topical Report prepared for the Gas Research Institute. GRI-97/0123, August.

Markstein, G.H., 1975. Scaling of Radiative Characteristics of Turbulent Diffusion Flames. National Fire Prevention and Control Administration.

Schefer, R., Houf, B., Bourne, B., Colton, J. 2004. Experimental Measurements to Characterize the Thermal and Radiation Properties of an Open-flame Hydrogen Plume. Presented at the 15th Annual Hydrogen Conference and Hydrogen Expo USA. April.

Stephens, M.J. 2000. A Model for Sizing High Consequence Areas Associated with Natural Gas Pipelines. Topical Report prepared for the Gas Research Institute. GRI-00/0189, October.

Turns, S.R. and Myhr, F.H. 1991. Oxides of Nitrogen Emissions from Turbulent Jet Flames: Part I—Fule Effects and Flame Radiation. Department of Mechanical Engineering. Combustion and Flame 87 pages 319 – 335.

Zabetakis, M.G. and Burgess, D.S. 1961. Research on the Hazards Associated with the Production and Handling of Liquid Hydrogen. TN23.U7 No. 5707.